EXHIBIT 13

Department of Regulatory and Economic Resources
Environmental Resources Management
701 NW 1st Court, 4th Floor
Miami, Florida 33136-3912
T 305-372-6700 F 305-372-6982

miamidade.gov

August 3, 2023

VIA ELECTRONIC MAIL: Brian.Accardo@fpl.com
A Paper Copy of This Correspondence Will Not Follow by Regular Mail.

Brian Accardo, P.E.,
Environmental Services Manager
Florida Power and Light
700 Universe Blvd.
Juno Beach, Fl 33408

Re: Florida Power and Light Remedial Action Annual Status Report (RAASR) dated November 15, 2022 and submitted on behalf of the Florida Power and Light Turkey Plant Facility and Cooling Canal System (HWR-851) located at, near or in the vicinity of 9700 SW 344 Street, Miami-Dade County, Florida

Dear Mr. Accardo:

The Department of Environmental Resources Management (DERM) has reviewed the referenced report received via email on November 15, 2022, along with supplemental information or clarifications provided on March 15, 2023, and April 28, 2023 and in multiple meeting with FPL's and DERM's technical teams. Please note that as a part of the review process, DERM's independent consultants peer reviewed and provided comments on the revised groundwater model as well as the Continuous Surface Electromagnetic (CSEM) Survey. The consultant's comments and recommendations are provided as an attachment to this correspondence. Staff comments are provided below:

Section 3: Groundwater Monitoring Data

1. Section 3.2 – Year 4 Water Quality Conditions and Trends

   DERM acknowledges the declining trend in chloride concentration observed in some monitoring wells since startup of the recovery well system and especially the shallow zone in wells west of the cooling canal system (CCS) and that the narrative of Section 3.2 indicates "three of the 22 wells have since transitioned during [recovery well system] RWS operations from hypersaline to saline." However, to provide enhanced clarity with respect to the system's performance in regard to the requirements of the Consent Agreement (intercept, capture, contain, and retract hypersaline groundwater) DERM recommends that the summary highlight for the section (highlighted box) include a statement indicating number of compliance wells that have transitioned from above to below hyper salinity during the reporting period.

2. Section 3.2.2 Intermediate and Deep Wells

a. The report indicates that "average tritium concentrations in the intermediate and deep wells for the reporting period range from 496 pCi/L (TPGW-19M) to 4,728 pCi/L (TPGW-15M), indicating varying degrees of CCS groundwater influence with concentrations in excess of 1,000 pCi/L within approximately 1 mile of the CCS." Provide the basis for the use of tritium concentration of 1,000 pCi/L as a point of reference.

b. The report offers the follow as a potential explanation for the increase in tritium concentration in TPGW-15M and TPGW-15D

   "The increases at TPGW-15M and TPGW-15D are likely related to RWS pumping as this well cluster is situated between the CCS and RWS-3 (RWS-3 is less than 0.5 mile northwest of the CCS). … It is suspected that groundwater from under the CCS may be pulled past TPGW-15 at depth, thereby increasing the percentage of CCS-sourced groundwater as reflected in higher tritium concentrations." and

   "Due to the proximity of TPGW-L3-58 to the TPGW-15 well cluster, it is also suspected TPGW-L3-58 could be similarly affected."

   Please note that the proffered explanation is not supported by the chloride concentrations in the TPGW-15M and TPGW-15D which would be expected to be similarly influenced by their position relative to the CCS and RWS-3. However, a statistically significant reduction has been observed in TPGW-15M with TPGW-15D indicating no trend. Additionally, TPGW-L3-58 is located over 1 mile from RWS-3 and likely isolated from the influence of RWS-3 by RWS-4 located 0.3 miles to the north.

3. Section 3.2.4

   DERM acknowledges the uncertainties and constraints associated with the use of groundwater monitoring data for evaluating compliance with the CA. However, within DERM's regulatory framework, the data provided by the monitoring wells is and will continue to be a critical component of any decision regarding whether or not compliance has been achieved.

Section 4: CSEM Survey

Peer review comments provided by DERM's consultant are provided as Attachment 1.

Section 5: Groundwater Model

Peer review comments provided by DERM's consultant are provided as Attachment 2.

4. Section 5.3 - Remediation Year 5 and 10 Forecast

a. The discussions regarding the groundwater model forecast versus the CSEM derived plume configuration shall include a table that provides the CSEM layers with their corresponding groundwater model layer.

b. Notwithstanding the differences between the AEM measured retraction and the groundwater model predictions, the data indicates recalcitrant hypersalinity in the deeper portions of the aquifer. Therefore, as provided in Section 17.b.iii of the Consent Agreement, consistent with the requirement of Section 20.c.v of the FDEP Consent Order, and as discussed in several meetings between FPL's representatives and DERM staff, the Year 5 RAASR shall provide a detailed evaluation of the effectiveness of the RWS to achieving the objective to retract the hypersaline plume, at all intervals, to the L-31E canal within 10 years (FDEP Consent Order) and recommendations for modifications to the RWS, the project components or system design to ensure the ability of the system to achieve the objectives of ultimately retracting the plume, at all intervals, to the L31E canal. The evaluation shall include projections, based on the system modifications proposed, for a timeline for achieving compliance with the above-stated requirement.

The Year 5 RAASR shall be submitted in accordance with the established timetables and shall address the comments provided herein as appropriate and applicable.

Please be advised that DERM has the option to collect split samples at any sampling event ; therefore, DERM shall be notified in writing via email, a minimum of three (3) working days prior to the implementation of any sampling or field activities. Email notifications shall be directed to DERMPCD@miamidade.gov, Luis.Otero2@miamidade.gov and Lorna.bucknor@miamidade.gov.
Please include the DERM file number (HWR-851) on all correspondence.

The consultant collecting the samples shall perform field sampling work in accordance with the Standard Operating Procedures provided in Chapter 62-160, Florida Administrative Code (FAC), as amended. The laboratory analyzing the samples shall perform laboratory analyses pursuant to the National Environmental Laboratory Accreditation Program (NELAP) certification requirements. If the data submitted exhibits a substantial variance from DERM split sample analysis, a complete resampling using two independent certified laboratories will be required.

Any person aggrieved by any action or decision of the DERM Director may appeal said action or decision to the Environmental Quality Control Board (EQCB) by filing a written notice of appeal along with submittal of the applicable fee, to the Code Coordination and Public Hearings Section of DERM within fifteen (15) days of the date of the action or decision by DERM.

Technical Reports (assessment, remediation, etc.) should be submitted via email to DERMPCD@miamidade.gov. For files too large for electronic transmittal, the public is requested to utilize Drop-Box or other equivalent FTP link. Please be advised that electronically submitted reports that require a Professional Engineer's (P.E.) or Professional Geologist's (P.G.) sign and seal shall be signed and sealed in accordance with the applicable portions of Chapter 471, Florida Statue (F.S.) and

Rule 61G15, Florida Administrative Code (FAC) for P.E.s and in accordance with Chapter 492, F.S. and Rule 61G16, FAC, for P.G.s.

If you should have any questions concerning the above, please contact me at wilbur.mayorga@miamidade.gov or contact Lorna Bucknor at lorna.bucknor@miamidade.gov.

Sincerely,

Wilbur Mayorga

Wilbur Mayorga, P.E., Chief
Environmental Monitoring & Restoration Division, DERM

attachments

ec: John Hampp, FPL, - John.Hampp@fpl.com
Scott Burns, FPL – Scott.Burns@fpl.com
Allan Stodghill FDEP - Allan.Stodghill@dep.state.fl.us
Lisa Spadafina, DERM Director
Craig Grossenbacher, Luis Otero, - DERM

ATTACHMENT 1

CSEM REVIEW COMMENTS

Memo

ARCADIS

SUBJECT
Final Review Memorandum for the Florida Power and Light 2022 Remedial Action Annual Status Report

TO
Wilbur Mayorga
Miami-Dade County DERM

DATE
June 2, 2023

OUR REF
30170232

COPIES TO
Lorna Bucknor – DERM
Greg Sitomer – DERM

FROM:
Patrick O'Connell
Monica Heintz
Gregory Byer

On behalf of Miami-Dade County Department of Environmental Resources Management (DERM), Arcadis U.S., Inc. (Arcadis) prepared this Final Review Memorandum (Final Review) to summarize Arcadis' review of the Florida Power and Light (FPL) Turkey Point Clean Energy Center, Remedial Action Annual Status Report, Year 4 (2022 RAASR; FPL 2022).

On March 1, 2023, Arcadis submitted an Initial Review Memorandum for the 2022 RAASR (Initial Memo, Arcadis 2023a). The key conclusion presented in the Initial Memo was that AGF utilized a flawed approach to calculate estimated AEM-resistivity thresholds associated with the chloride concentration that defines hypersalinity, 19,000 mg/L, as indicated in the Consent Agreement (Miami-Dade County 2015). AGF calculated AEM-resistivity threshold values that showed a monotonic decrease over time. However, this trend appears to be related to the inclusion of data from outside the relevant calibration range to establish the relationships between chloride concentration, water resistivity, and AEM-resistivity. The erroneous decreasing trend in the AEM-resistivity threshold value resulted in unreliable estimates of hypersaline volume over time and an unexpected pattern in apparent remedial system performance being reported in the 2022 RAASR.

On March 15, 2023, Scott Burns at Florida Power and Light (FPL) emailed questions and comments regarding the Initial Memo to Wilbur Mayorga and Lorna Bucknor of DERM and on March 29, 2023, Arcadis provided a response memo (Arcadis 2023b), including supporting files detailing the data and analysis methods used in the Initial Memo (Arcadis 2023a) to evaluate the conclusions of the 2022 RAASR. On April 28, 2023, FPL provided a proposed path forward and a report titled Turkey Point Remediation Project Alternate Regression Modeling and Data Processing Report by Dr. Kirk Cameron (Cameron 2023). In this report, Dr. Cameron confirmed that the monotonic drift in the AEM-resistivity threshold values calculated by AFG is an artifact, and that (with the exception of 2018) year-over-year AEM-resistivity threshold values are similar and do not trend in a single direction with time. Additionally, Dr. Cameron suggested changes to the regression procedure, including:

- Using a one-equation approach, directly relating chloride concentrations measured in monitoring wells and estimated AEM-resistivity values at the same locations rather than relating AEM-resistivity to water resistivity and water resistivity to chloride concentrations. Results from the one-equation approach are comparable to those from the two-equation approach and using only one equation substantially simplifies calculation of AEM-resistivity threshold values and the associated uncertainty.
- Appling the Deming regression approach to account for error in both chloride concentrations and AEM-resistivity threshold values.
- Combining data across years to calculate a single AEM-resistivity threshold.
- Using a bootstrap approach to estimate the 95 percent confidence interval around the mean AEM-resistivity threshold value.

Each of these changes are acceptable. However, in his report Dr. Cameron continued to use data from outside the calibration range (less than 10,000 mg/L) to develop the regression, resulting a substantial decrease in the estimated AEM-resistivity threshold relative to those calculated by Arcadis using data associated with chloride concentrations greater than 10,000 mg/L.

In conjunction with review of FPL's proposed path forward and Dr. Cameron's report, Arcadis reexamined the combined data set, including data collected at each of the monitoring wells between 2018 and 2022 and demonstrated that inclusion of data associated with chloride concentrations less than 10,000 mg/L from shallow wells results in a statistically significant change in the slope of the regression relating chloride concentrations to AEM-resistivity values (Arcadis 2023c). Because the overwhelming majority of the relevant hypersaline volume occurs at depths represented by the intermediate and deep wells (Layers 9 through 14), the AEM resistivity and chloride concentration relationship observed at in the intermediate and deep wells defines the primary data set of interest. Including the subset of shallow data that is outside of the primary data set of interest results in lower estimates of the AEM-threshold value. This results in underestimation of the hypersaline volume. Based on these findings, as detailed in the May 16, 2023, Response to April 28, 2023, Correspondence from FPL (Arcadis 2023c):

- Data associated with chloride concentrations greater than 10,000 mg/L will be included in the calibration of AEM-resistivity to the 19,000 mg/L chloride hypersalinity threshold, unless there are multiple lines of evidence to indicate that a particular result is faulty.
- Inclusion of data from intermediate and deep wells with chloride concentrations less than 10,000 mg/L is acceptable.
- Inclusion of data from shallow wells with chloride concentrations less than 10,000 mg/L is not acceptable.

Based on evaluations conducted and correspondence exchanged over the 2022 RAASR review period it is demonstrated that the AEM-resistivity threshold values calculated by AGF and presented in the 2022 RAASR are erroneous to a degree that meaningfully influences the estimation of hypersaline volume and extent. As a result, the following elements of the 2022 RAASR are considered to be inaccurate:

- All AEM-resistivity hypersalinity thresholds,
- All hypersalinity volume estimates across years between 2018 and 2022,
- The percent change in hypersalinity year-over-year, and relative to baseline,
- The location and orientation of the interpreted 19,000 mg/L contour or otherwise indicated lateral areas of hypersalinity.

As a result of these inaccuracies, statements indicating that westward expansion of the plume has been halted and that the objectives of the Consent Agreement and Consent Order are being met through Year 4 may be true, but have not been adequately evaluated in the 2022 RAASR. Reanalysis across the years between 2018 and 2023 in a manner consistent with Arcadis's responses to FPL's proposed path forward (Arcadis 2023c) will be conducted as a component of FPL's Year 5 progress report, in 2023. Arcadis agrees with the factors for additional evaluation in the Year 5 report presented in 2022 RAASR Section 4.3.6, and these should also be included in the Year 5 report.

The following sections of the 2022 RAASR are fundamentally flawed and/or their relevance has been eliminated based on Dr. Cameron's statistical analysis reevaluation and methodology recommendations:

- RAASR Section 4.2.3
- RAASR Section 4.2.4
- RAASR Section 4.3.2
- RAASR Section 4.3.3
- RAASR Section 4.3.4
- RAASR Section 4.3.5
- RAASR Appendix G Executive Summary points 2.2 through 2.8
- RAASR Appendix G Executive Summary points 3.1 and 3.2
- RAASR Appendix G Section 3
- RAASR Appendix G Section 4 points 4.1.2 through 4.1.8, 4.2.1, and 4.2.2

Because these components are not applicable in their current form, each of the specific technical errors are not enumerated in this Final Review. The following subsections of this Final Review detail comments on the remaining RAASR components and reiterate the importance of removing high-frequency noise in AEM data and properly quantifying the uncertainty in the modeled resistivity data using available metrics. These steps are aimed at providing a more accurate estimation of the AEM-resistivity threshold and evaluate meaningful changes in resistivity at any given location between years.

Additional 2022 RAASR Comments

Section 1.4 Independent Technical Review

- FPL states "Six alternative evaluation approaches for assessing hypersaline plume volume estimates from 2018 and 2019 (Year 1 of remediation) were conducted by Arcadis using FPL AEM data. These alternatives produced a range of plume reduction values for the first year of RWS remediation from 16% to 25%, with Arcadis' estimated Year 1 plume volume reduction of 24%; this compared well with FPL's Year 1 volumetric reduction report of 22% (Arcadis 2020). The Arcadis evaluation of alternative methods indicates FPL's methods for calculation of changes in plume volume are consistent with these alternative methods."
  - This statement does not match the volumes that were presented in Appendix G of the 2022 RAASR.
- FPL states "Arcadis's review of the approach FPL uses to assess uncertainty surrounding the regressions that ultimately relate AEM-resistivity to chloride concentration focused on how that uncertainty potentially relates to chloride estimation error on a point-by-point scale."
  - Arcadis's review did not focus on chloride estimation error on a point-by-point basis, but rather discourages point-by-point calculation of chloride concentrations in favor of establishing the range of values that are representative of the mean AEM-resistivity value associated with the hypersalinity threshold value of 19,000 mg/L.
- FPL states "the use of the resulting confidence interval surrounding the regression does not fully represent the range of possible predictive chloride values at any 19,000 mg/L estimated value in the study area."
  - The confidence interval represents the range across which the mean AEM-resistivity value associated with the 19,000 mg/L hypersalinity threshold will occur at a specified level of confidence. Prediction limits are used to represent the range of possible values and are wider than confidence intervals. The idea is

not to establish the range of “predictive chloride values”, but to establish the range of AEM-resistivity values that represent the mean threshold value at a specified level of confidence.

Section 3 Groundwater Monitoring Data

- Note that the summary paragraph does not indicate what there is a declining trend in. Presumably chloride.
- On figures showing chloride concentrations over time, like those presented in Appendix E, please put all (or at least most) wells on the same scale and add a horizontal indicator line for the hypersalinity threshold (19,000 mg/L).
- Although statistically significant decreasing trends demonstrate that conditions are improving, the magnitude of this improvement has not been examined to determine if it is comparable to what is needed to achieve the Consent Order goal of (as stated in the 2022 RAASR) reduce the westward extent of the hypersaline plume to the L-31E canal within 10 years.
  - FPL should evaluate the magnitude of statistically significant decreasing trends at wells with hypersaline concentrations to evaluate if chloride concentrations are projected to be less than 19,000 mg/L at wells west of the L-31E Canal by 2028. This can be achieved by coupling Sen’s Slope (Theil-Sen Line) with Mann Kendall. If a parametric method (e.g., linear regression) is used to evaluate if the magnitude of the trend is sufficient to achieve the goal, then the fit of the data to the selected model should be considered and discussed.
- FPL states “Based on a review of the data, there appears to be relatively few meaningful salinity trends other than a statistically significant declining trends in chloride, tritium, and salinity at TPGW-5M over the reporting period”.
  - Concentrations of chloride at TPGW-5M have been less than the hypersaline threshold over the full monitoring period, and therefore the trend is not really meaningful in the context of the Consent Agreement objectives.
- FPL states “Chloride reductions in the compliance area in the middle well at TPGW-5, which is over 3 miles west of the RWS, is an indication of the lateral reach of the withdrawal system”.
  - This is an over interpretation of the influence of the extraction system given that the only well with a trend has not been hypersaline.
- Titles on Figures 3.3-4 through 3.3-6 should indicate Year 4 rather than Year 3.

Section 4 Continuous Surface Electromagnetic Mapping Survey Summary

- Because this is a quantitative, spatio-temporal assessment, there are inherent challenges which need to be addressed concerning the year-to-year variations. Munday et al (2010) and Munday and Sorensen (2018) examined the use of AEM for spatio-temporal assessments of changes in electrical conductivity at differing dates. Munday et al (2010) lays out the case for developing a means for identifying and quantifying variability at differing dates in the data collected and instituting correction to remove biases introduced by the data collection process. To date, AGF (2018) through AGF (2022) have not properly addressed this concern about temporal variation. That is, there has been no effort to establish a ***quantitative*** means to perform an independent check to verify year-to-year comparability in the raw and modeled AEM data. It should be noted that the need for recognition of year-to-year bias in the raw geophysical data and the imposition of a correction to the raw geophysical data prior to modeling, is an essential step. Quoting Munday and Sorensen (2018),

We emphasize the need for caution when considering the observed spatial variations, stressing the importance of understanding and accounting for system investigation depth and the potential for artefacts that might be introduced from noise, system geometry and/or data interpretation procedures. These issues should always be borne in mind when comparing data and derived conductivity models from different dates.

Arcadis has spoken with the technical experts at Aarhus (Bjarke Roth and Toke Højbjerg Søltoft, pers. comm.) about the application of the SkyTEM system to similar time lapse problems and it was indicated to Arcadis that this scenario is unprecedented. The burden is on FPL to provide direct evidence that an independent quantitative analysis and check has been performed which assures that the AEM raw data and subsequent data processing and inversion modeling are truly comparable from year to year with data obtained at the project site. The best practice for demonstrating comparability from year to year should be a sound empirical set of tests where the results are compared to a standard, non-time-varying, reliable measure of resistivity. Sources of data, taken in a location that is demonstrably stable in its resistivity from year to year, which can be used in testing comparability include induction conductivity logs, groundwater conductivity data measured concurrent with logging and AEM data collection, the raw AEM voltage and altitude data, and inversions modeling results. For example, Arcadis suggested a year-to-year comparison of AEM derived resistivity values in an area where variation in resistivity values associated with the on-going remediation would be expected to be minimal, confirmed by borehole geophysical and groundwater electrical conductivity (resistivity) data (Arcadis 2020 Section 2.2.2.3 Evaluation of Potential Systematic Bias of Modeled Resistivity Values).

- The 2018 through 2022 borehole geophysical results are similar year-to-year, particularly in the depth intervals that correspond with the medium and deep well screens, which are most relevant to assessing the hypersaline plume extent. In fact, 2018 through 2022 induction conductivity results are nearly indistinguishable in the lower half of the logged interval (nominally 12.5+/- 2.5 meters to total depth, typically less than 35 meters depth). In the upper half of the logged interval (0 to 12.5 +/- 2.5 meters depth, corresponding to the shallow (S) screens), there is greater separation in the year-to-year resistivity values of the individual logs. Notably, groundwater in the shallow screened interval is generally not reflective of the hypersaline plume associated with the site. The individual year-to-year logs show similar patterns with depth in the zone which corresponds to the shallow aquifer screens, and the data is mainly shifted in resistivity left or right from a notional baseline. Notably, the maximum difference at any depth in the upper half of the borehole is generally not more than 10 ohm-meters. It is Arcadis's view that the AEM modeling results should reflect a similar degree of year-to-year relative variation as the borehole geophysics, even if the values in the AEM and borehole geophysics differ in absolute terms. However, this is not what **Figures 2-20, 2-22, 2-24, 2-26, 2-28, 2-32, 2-34, 2-36, and 2-38** reflect, especially in the medium (M) and deep (D) screened intervals. FPL has not adequately accounted for the differences in year-to-year variance between the induction conductivity log data and the AEM-based modeled resistivity data where the variance in the induction conductivity in the M and D wells is generally much lower than the variance in the AEM-based modeled resistivity data.
- FPL continues to use the phrase "statistical range in bulk resistivities" in the selected 175-m radius over which sounding results are averaged. If this phrase is used in the Year 5 report, "statistical range" needs to be defined.

- No mention is made in the RAASR (2022) of the discussion in Section 2.5 of the AGF (2022) report about the comparability of 1) the radial technique of calculating average resistivities based on the closest AEM soundings and 2) gridding each inverted SCI model layer with minimum curvature. Results were shown on Figure 2-18 of AGF (2022), and Arcadis agrees that the results between methods are similar. Arcadis suggests that because gridded minimum curvature method provides comparable results with radial technique that this method should be used to estimate AEM resistivity values at locations previously left out of the threshold calibration analysis due to lack of soundings within the 175-foot radius. The wells that should be included are: TPGW-4, TPGW-12, and TPGW-15.
- The comparison of measured and calculated chloride concentrations at monitoring wells (Table 4.2-3) is a flawed method for evaluating the regression because the same data are used to develop the regression and make the comparison. This type of evaluation should not be included in the Year 5 report.
- The Discussion of Findings (Section 4.3) begins with a discussion of the natural occurrence of hypersaline water. However, it remains unclear from the text where this naturally occurring hypersaline water is apparent in site data or what the implication is. Please make these elements clear if this is to remain the first point of discussion of findings.

Arcadis did not review 2022 RAASR Sections 5 (Groundwater Model) and 6 (Cooling Canal System Management).

Uncertainties Associated with Electrical Resistivity

The calibration relationships and resulting volume estimates are sensitive to small differences in AEM-resistivity estimates; therefore, it is prudent to recognize and reduce random and systematic noise in the AEM data to the greatest extent practicable before extracting estimates to use in the calibration to the hypersalinity threshold. In the Initial Memo and subsequent submittal (Arcadis 2023a and 2023b), Arcadis observed that there is residual, high-frequency noise in the resistivity data. This high-frequency variability appears to be noise inherent in the data acquisition and processing because it is random and unrelated to the year-to-year changes in groundwater chemistry. Arcadis (2023a and 2023b) provided an empirical analysis of a subset of the modeled resistivity data. However, Arcadis has ongoing concerns about the sources of the noise and related uncertainties associated with the AEM data in general. The 2022 RAASR Section 4.2.4, Sources of AEM Method Uncertainty, frames the uncertainty associated with the AEM bulk resistivity around the measured chloride levels in monitoring wells relative to estimates of pore water chloride level derived from AEM-estimated chloride regressions. It is suggested by FPL that the differences are caused by factors including:

- Geologic Noise[1].
  - Spatial variations in porosity introduce error since the assumption is that porosity is constant is imbedded in the regression model.
- Spatial Displacement of Samples.
  - AEM soundings are not co-located with monitoring wells due to the interferences caused by the wells in the AEM data.

---

[1] Note that a geological variable that is omitted from the discussion is the effect of changes in the water chemistry related to the mixing of various surface and groundwater types such as sodium chloride dominated (seawater or CCS waters) or calcium bicarbonate dominated (fresh groundwater hosted by carbonate aquifers).

- Vertical dimensions of screened intervals in wells are not aligned with the AEM layer boundaries and in some cases span across the boundary between two layers.
- Samples from monitoring wells come from a discrete point on the scale of a meter while AEM resistivity is resolved on the scale of 10s to over 100 meters, although it is noted that changes in pore water chloride content ought to be smooth over the distance of 10s of meters.

Although the factors noted above would be expected to introduce uncertainty in correlating bulk resistivity with chloride concentration, there is no mention of the error associated with the measurement of the raw TEM voltage data and the subsequent processing and inversion modeling of the voltage data into depth-resistivity models.

Automatic and manual data processing endeavor to remove or minimize noise in the AEM voltage data introduced by capacitive and galvanic couplings as well as positional and orientation errors during data collection. However, errors associated with the data inversion process also exist. The inversion modeling process is an attempt to approximate the true earth resistivity structure with a smooth 1-dimensional model consisting of layers of fixed thicknesses that increase steadily with depth. Assumptions are also made about the constraints placed on the modeling process in the lateral and vertical variations in resistivity values to allow for a 2-dimensional spatially constrained inversion (SCI) process.

Not mentioned in the 2022 RAASR, but briefly mentioned in Section 2.4.6 of the 2022 AGF report, are data quality related measurements that are output from the SCI process. These include data residuals, total residuals, depth of investigation, and standard deviation factor. AGF (2022) states in Section 2.5, paragraph 1,

> *One of the key items in 'accepting' the data (i.e., accepting the quality of the data) and verifying the resistivity model is the inspection of the data residuals from the inversion and the comparison of the resistivity structure in the inversion to borehole induction logs. As mentioned above, Figure 2-17 is a plot of the data residual from the final Spatially Constrained Inversion and Figure 2-16 is a histogram of the data residuals from the SCI. The distribution is roughly 'normal' around approximately 0.61 indicating that there are no problems with outliers or other biases. A detailed description of the calculation of the residual within the Aarhus Workbench can be found in Christensen, Reid, and Halkjaer (2009).*

The qualitative statement that the data residual distribution with a median value of 0.61 indicates no problems with outliers or other biases does not provide a quantitative statement of uncertainty that is useful for evaluating confidence in individual resistivity values which are derived from the inversion modeling process. Figure 2-17 in AGF (2022) is a depiction of the data residuals, although nothing is done further to include the residuals into the evaluation of the uncertainties surrounding the resistivity models. The data residuals and depth of investigation are shown graphically, for example, in Figure 2-13 in AGF (2022). However, there is no corresponding, quantitative demonstration of uncertainty in the resistivity of individual layers by providing the data residual plot for the entire sounding model.

AGF (2022) does briefly discuss a metric, namely the standard deviation factor, which potentially provides insight into the uncertainty associated with the resistivity model values on a layer-by-layer basis. The standard deviation factor (STDF) is described in Section 2.4.6 of AGF (2022) as follows,

> *For each layer a resistivity (Rho_I) and a Resistivity Standard Deviation (Rho_I_STD) is calculated. This value represents the one standard deviation factor range of the resistivity that is equally valid at that point. The resistivity value multiplied and divided by that number provides the range of statistically valid values for that resistivity and layer. More information on the calculation can be found in Auken et al. (2005). These data are included in the data deliverables described below in Section 5.0.*

AGF (2022) does not address uncertainties associated with modeled resistivity data beyond providing the statement above and noting the STDF data is included in the inversion modeling output file.

Arcadis reviewed the relevant reference[2] to better understand the relevance of the standard deviation factor and how it might be applicable to this project. Under the heading of "Analysis of model estimation uncertainty" in Auken & Christiansen (2004), quoting:

> *Standard deviations on model parameters are calculated as the square root of the diagonal elements in C_{est}. For mildly nonlinear problems this is a good approximation. Because the model parameters are represented as logarithms, the analysis gives a standard deviation factor (STDF) on the parameter q_s, defined by*
>
> $$STDF(q_s) = \exp\left(\sqrt{C_{est(s,s)}}\right) \qquad (30)$$
>
> *Hence, under a lognormal assumption, it is 68% likely that a given model parameter q falls in the interval*
>
> $$\frac{q}{STDF_q} < q < q \cdot STDF_q \qquad (31)$$
>
> *Thus, the impossible case of perfect resolution has an STDF of one. An STDF of 1.1 is approximately equivalent to an error of 10%. Moderate to well-resolved parameters have an STDF less than 1.5, poorly resolved parameters an STDF less than 2, and mainly unresolved parameters an STDF greater than 2.*

Arcadis applied the STDF to the resistivity values found in the file "TurkeyPoint_2022_SCI2_Inv.csv" provided in Appendix 8 of AGF (2022). The resistivity values are assumed to be the q model parameter in this case. As stated above, there is a 68% likelihood that the resistivity value falls in the range between the quotient and product of resistivity to STDF. Because this is a lognormal distribution, this is equivalent to saying the natural log of resistivity [ln(R)] has a 68% likelihood of falling between the difference and sum of ln(R) and ln(STDF).

To illustrate the results of the computation of the 68% intervals for resistivity, see **Figures 1 and 2 (Attachment A)**, which are plots of the data from Line 104501 for Layers 10 and 13 for 2022. Also shown on these plots is the graph of the STDF and the qualifications based on the STDF in terms of how well or poorly resolved the parameters are as noted above in the quote from Auken & Christiansen (2004).

Arcadis brings this matter to FPLs attention as we believe this requires further discussion and explanation. If FPL agrees that Arcadis has correctly interpreted the application of the STDF as a valid metric for quantifying the uncertainty in the resistivity model values, then incorporation of the uncertainty ranges quantified with the STDF for each layer should be a part of the overall uncertainty analysis in combination with the uncertainties associated with estimating the AEM-resistivity hypersalinity threshold. If Arcadis has misinterpreted the meaning of the STDF metric, we would appreciate an explanation of how this metric should and will be properly applied to the data from this point forward.

[2] The relevant reference was incorrectly cited as Auken et al. (2005) and is actually Auken & Christiansen (2004).

References

AGF. 2018. Report on Advanced Processing and Inversion of 2018 AEM Survey Data and Derived Chloride Concentrations near the Turkey Point Power Plant, Southern Florida. June 8, 2018.

AGF. 2019. Report on Advanced Processing and Inversion of 2019 AEM Survey Data and Derived Chloride Concentrations near the Turkey Point Power Plant, Southern Florida. July 23, 2019.

AGF. 2020. Report on Advanced Processing and Inversion of 2020 AEM Survey Data and Derived Chloride Concentrations near the Turkey Point Power Plant, Southern Florida. December 18, 2020.

AGF. 2021. Report on Advanced Processing and Inversion of 2021 AEM Survey Data and Derived Chloride Concentrations near the Turkey Point Power Plant, Southern Florida, Revised. August 17, 2021.

AGF. 2022. Report on Advanced Processing and Inversion of 2022 AEM Survey Data and Derived Chloride Concentrations near the Turkey Point Power Plant, Southern Florida, Revised. September 21, 2022.

Arcadis. 2020. Review of Aerial Electromagnetic Surveys at Turkey Point Power Plant, Southern Florida. October 28.

Arcadis. 2023a. Initial Review Memorandum for the Florida Power and Light 2022 Remedial Action Annual Status Report.

Arcadis. 2023b. Response to Florida Power and Light Questions and Comments emailed March 15, 2023. March 29.

Arcadis 2023c. Response to April 28, 2023 Correspondence from Florida Power and Light. May 16, 2023.

Auken, E., & Christiansen, A. V. (2004). Layered and laterally constrained 2D inversion of resistivity data. Geophysics, 69(3), 752-761.

Auken, E., Christiansen, A.V., Jacobsen, B.H., Foged, N., and Sørensen, K.I., 2005, Piecewise 1D laterally constrained inversion of resistivity data: Geophysical Prospecting, v.53, p.497-506.

Cameron, Kirk. 2023. Turkey Point Remediation Project Alternate Regression Modeling and Data Processing Report. April 26.

FPL. 2022. Turkey Point Clean Energy Center Remedial Action Annual Status Report Year 4. November 15.

FPL and Stantec. 2020. Turkey Point Clean Energy Center Remedial Action Annual Status Report Year 2, Part 1. November 13.

Miami-Dade County. 2015. Miami-Dade County, Department of Regulatory and Economic Resources, Division of Environmental Resources Management v. Florida Power & Light Company. Consent Agreement. October

Munday, T.J., Fitzpatrick, A., Berens, V., Viezzoli, A. and Cahill, K., (2010). Spatio-Temporal Monitoring with Airborne EM Data - Still Wishful Thinking, or a Realistic Proposition? *Symposium on the Application of Geophysics to Engineering and Environmental Problems 2010, Keystone, Colorado*, 277-286.

Munday, T.J. and Soerensen, C., (2018). Resolving Changes to Freshwater Lens Systems in a “Sea of Salinity” using Multi-date Airborne EM. *ASEG Extended Abstracts 2018*, 1-8.

Attachment A. Figures

Attachment A

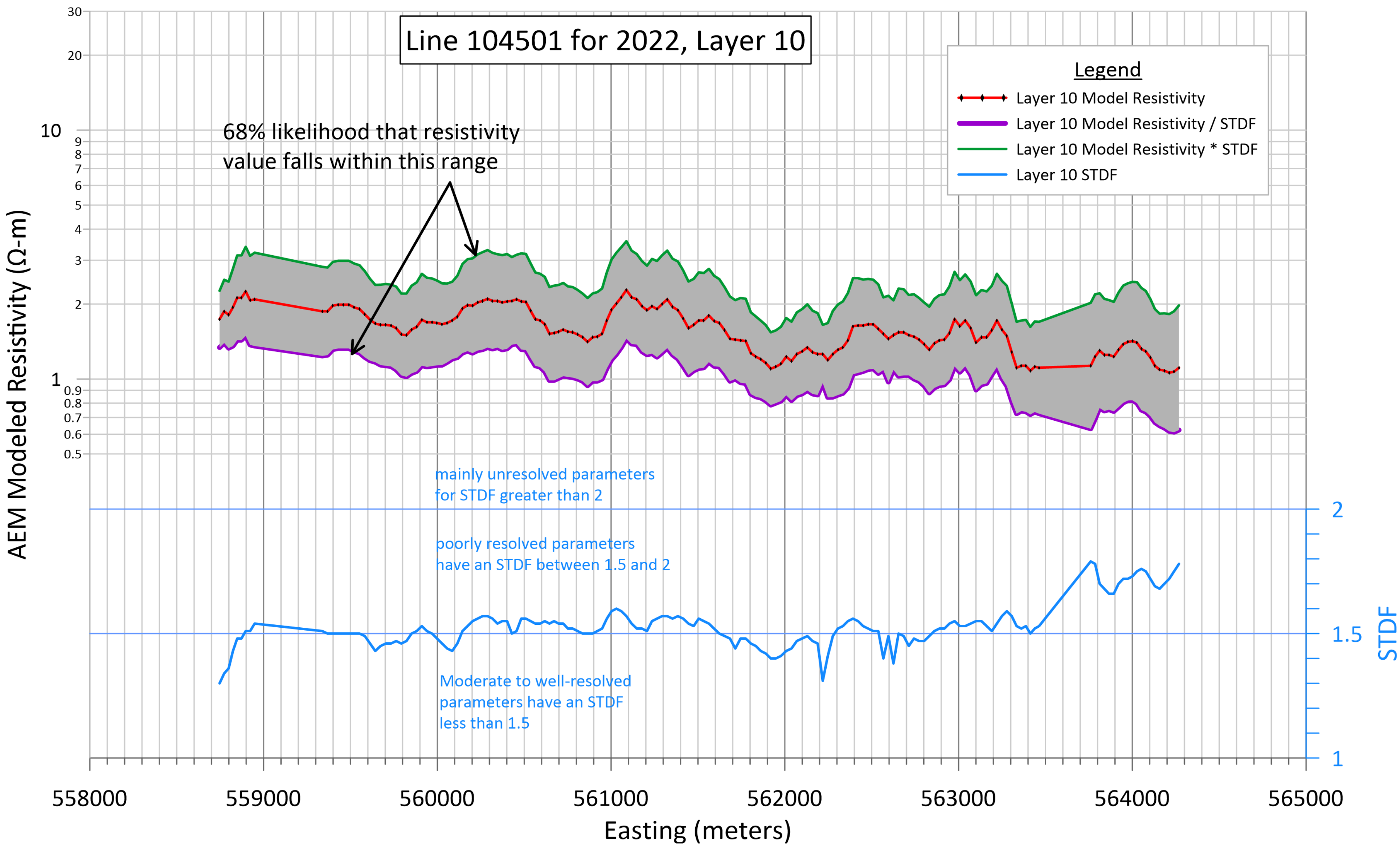

Notes:

STDF = Standard Deviation Factor

Model Resistivity / STDF = lower limit of 68% likelihood of resistivity for a lognormal distribution

Model Resistivity * STDF = upper limit of 68% likelihood of resistivity for a lognormal distribution

Data used for this plot was found in ***TurkeyPoint_2022_SCI2_Inv.csv*** which was part of the Data Deliverable in AGF (2022)

Documentation of the procedure for calculating the upper and lower limits and the description of the STDF ranges was found in Auken & Christiansen (2004)

FINAL REVIEW MEMORANDUM FOR THE FLORIDA POWER AND LIGHT 2022 REMEDIAL ACTION ANNUAL STATUS REPORT

EXAMPLE PLOT OF MODEL RESISTIVITY AND CALCULATED STDF-BASED LIMITS, LINE 104501, LAYER 10, 2022 DATA

ARCADIS

FIGURE
1

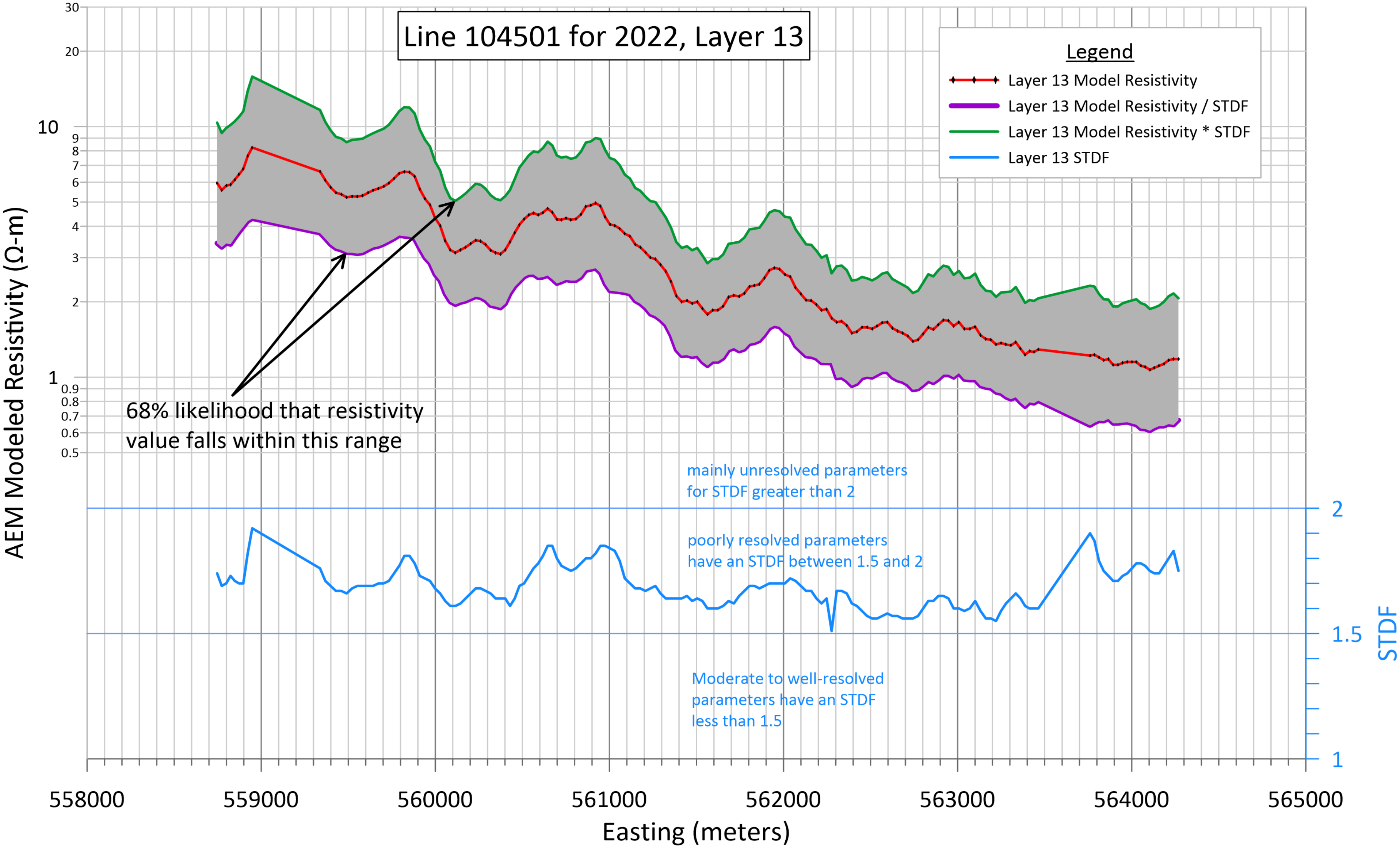

Notes:

STDF = Standard Deviation Factor

Model Resistivity / STDF = lower limit of 68% likelihood of resistivity for a lognormal distribution

Model Resistivity * STDF = upper limit of 68% likelihood of resistivity for a lognormal distribution

Data used for this plot was found in ***TurkeyPoint_2022_SCI2_Inv.csv*** which was part of the Data Deliverable in AGF (2022)

Documentation of the procedure for calculating the upper and lower limits and the description of the STDF ranges was found in Auken & Christiansen (2004)

FINAL REVIEW MEMORANDUM FOR THE FLORIDA POWER AND LIGHT 2022 REMEDIAL ACTION ANNUAL STATUS REPORT

EXAMPLE PLOT OF MODEL RESISTIVITY AND CALCULATED STDF-BASED LIMITS, LINE 104501, LAYER 13, 2022 DATA

ARCADIS

FIGURE 2

ATTACHMENT 2

GROUNDWATER MODEL REVIEW COMMENTS

Review of FPL's RAASR Year 4 and The Variable Density Groundwater Flow and Solute Transport Model (v7)

Prepared for

Division of Environment and Resources Management

Miami-Dade County, Florida

Groundwater Tek Inc.

Naples, Florida

March 20, 2023

Table Contents

Executive Summary

Groundwater Tek Inc. (GTI) was retained by the Miami-Dade County Division of Environment and Resources Management (Miami-Dade DERM) to evaluate the site-specific variable density groundwater flow and solute transport model developed by Florida Power & Light Company (FPL) and to assess the third-year performance of the remediation system to determine whether or not the remedial objectives could be met as specified in the Miami-Dade County Consent Agreement (MDC CA)(MDC, 2015).

The model was developed by FPL using the USGS computer code SEAWAT. Model simulations were used to develop a schedule for the mitigation and subsequently, to evaluate the effectiveness of a recovery well system (RWS) at mitigating saltwater contamination of the Biscayne Aquifer resulting from the saline water present in the FPL's Cooling Canal System (CCS) at its Turkey Point Nuclear Power Plant in Southern Miami-Dade County.

Scope of Work

Under a consent agreement between FPL and Miami-Dade DERM (2015), FPL installed a groundwater remedial system in 2018 to retract the hypersaline plume in the Biscayne aquifer to FPL's property boundaries by 2028. FPL has also developed a coupled variable density groundwater flow and salt transport model using USGS SEAWAT for the design and assessment of the remedial system.

Groundwater Tek Inc. has been retained to review the SEAWAT model versions v3 through v6, and FPL's first three annual progress reports (RAASR) for 2019 (Yr 1), 2020 (Yr 2) and 2021 (Yr 3). This review work is, as a continuation of the previous work, to review the latest version of FPL's SEAWAT model (v7) and its fourth-year progress report (RAASR for Yr4).

The following tasks will be performed for the review:

- Review of FPL's RAASR Yr4 report
- Review of FPL's SEAWAT model v7 (Appendix I)
- Review of Groundwater monitoring data
- Salt extraction data and modeling results
- Assessment of CSEM data and plume reduction
- Verification of SEAWAT model runs (Calibration, prediction, and sensitivity analyses)
- A technical report summarizing the findings, comments, conclusions and recommendations.

Work Performed

The following work elements were completed by GTI in this review:

(1) Model verification: the calibration and prediction models and sensitivity simulation provided in November 2022 by FPL;

(2) Review of groundwater monitoring data;

(3) Review of salt extraction data and modeling results;

(4) Review of the progress of the hypersaline plume retraction;

(5) Review of sensitivity simulation using 2022 CSEM-based initial salinity condition;

(6) Review of sensitivity simulation of L31-E Canal as a drain;

(7) Review of FPL Remedial Action Annual Report (RAASR) Year 4;

(8) Review of SEAWAT model version 7: the updates and model recalibration.

Findings and Conclusions

(1) The current RWS is making progress as indicated by CSEM survey data and groundwater monitoring data. About 9.24 billion pounds of salt has been removed from the aquifer since the beginning of the RWS operation and approximately 2.37 billion pounds of salt was removed in this report time period. The progress is more pronounced for the shallow and middle portions of the aquifer. The CSEM survey data from 2018 to 2022 indicated that the expansion of the hypersaline plume has been halted or reversed in the shallow portion of the aquifer. Water quality data from groundwater monitoring wells, also showed the decline of chloride concentration at many monitoring well sites.

(2) The major change of FPL SEAWAT model version 7 from previous versions is the increase of vertical resolution by splitting the deeper model layers. The current model has 17 layers, increased from 11 layers in previous models. The deep high flow zone in the previous models is split to the upper portion and the lower portion of the deep high flow zone. The increase of model layers helps more accurately locate the screens of monitoring wells and extraction wells. However, the increase of the model layers does not appear to change the overall picture of the model simulations. The most prominent difference appears to be at TPGW-1 in model layer 13 (Layer 10 in previous models), where simulated plume extent is much closer to the L-31E canal based on the current version of SEAWAT model.

(3) Based on the provided calibration statistical summary for this version of the SEAWAT model, the model has been reasonably well-calibrated to the calibration targets. The model was developed with good modeling practices. The model has gone through a number of steps of calibration against the data from many years. Automatic calibration tool (PEST) was implemented to facilitate the model calibration. The calibration targets include water levels, salt concentration, CSEM survey data, historical saltwater intrusion freshwater/saltwater interface, and monthly salt extraction rates. The model-predicted water levels, monthly salt extraction rates, and salinity in most of monitoring wells as well as selected CSEM survey data were in close agreement with the observed data. The solute transport calibration has room for improvement in future model

calibration. The model-predicted salinity values at some of the monitoring wells are not in close agreement with field measurements.

(4) Further model calibration with focus on the historical salinity match is necessary. The match between modeled and observed data at a number of monitoring wells is not satisfactory and needs to be improved. Modeled and CSEM-based plume extents in deep aquifer are not in close agreement for May 2018, which presented an initial mass concentration distribution. The results from the sensitivity analysis indicate that externally generated initial mass conditions may not work well with prediction model, so a set of simulated initial conditions (heads, mass and temperature) may be necessary for prediction model improvement.

(5) The current version of SEAWAT model did not match the plume extents in the deep layers, representing the deep portion of the Biscayne aquifer. Comparison of modeled plume extent after model calibration and the CSEM-based plume extents in deep model layers indicate that the model is not able to match the field conditions for May 2022, which represent the initial condition for the prediction model.

(6) The model's inability for prediction of future change of the hypersaline plume remains as the major concern. The model did not match the plume in deep layers as of the end of May 2022 and the current model prediction indicates the hypersaline plume in the deep portion of the aquifer would not be retracted to the FPL's property by May 2028.

(7) The modeling results from the sensitivity simulation indicate that the hypersaline plume unintuitively expands westward in model layer 16, which is contrary to the conceptual model, and it is not supported by the CSEM survey data. On the other hand, this sensitivity simulation provides useful information that may allow us to identify some problems in the current conceptual model. The results of the sensitivity analysis may suggest that externally generated initial mass concentration may not hydrodynamically balanced with the model. Therefore, efforts to match the salinity distributions prior to the operation of the RWS (April 2018) may be critical to improve the model's ability for prediction. If the model cannot match the salinity distribution in April 2018, it will be very difficult to be used to predict the fate of the hypersaline plume with reasonable confidence.

(8) TPGW-18 is located at the edge of the hypersaline plume so the change of salinity at this location is a valuable indicator of the effectiveness of the RWS. So far, the water quality data from this well has not shown a convincing trend in the middle and deep sections. The chloride concentration contour maps, based on measured chloride concentrations have indicated the plume retraction is slightly behind at TPGW-18 and TPGW-22 in deep aquifer. The changes of salinity in the vicinity of TPGW-18 and TPGW-22 need to be closely watched. Although data from these two points may not be representative of the entire progress of remediation, they do provide critical data to provide us with the first hand of break-through curves showing the retraction of the plume in the deep aquifer.

(9) FPL has performed a sensitivity analysis to investigate the hydrological impact of L-31E Canal to the RWS system by modeling the canal as a drain rather a river feature. The results indicate the plume retraction are not significantly different for the shallow and middle portions of the aquifer. The results of this sensitivity analysis suggests that remedial efficiency of the RWS wells may be sensitive to the availability of water from the shallow layers above. The impact to the hypersaline plume is weaker at deeper depth such as model layer 16.

(10) The salt extraction rate is a direct indicator of the efficiency of the RWS. The modeled monthly salt extraction rates have been in close agreement of published data from 2018 to 2022. The simulated monthly salt extraction rate has been relatively statable over the last four years at about 140 million pounds per month. As the remediation continues, a decline of the monthly salt extraction rate is expected when the shallow and middle of the aquifer become less salty. It is not clear at this point why the salt extraction rate was relative stable yet the salinity in the shallow and middle portions of the aquifer declined over time. One possible explanation is that the RWS mainly extracts salt from the deeper portion where the hypersaline conditions remain. This would be the ideal situation when the RWS are removing the hypersaline plume west of the CCS but not from the CCS area. Identification of the sources of water feeding the RWS wells may help us understand the fate of the hypersaline plume and efficiency of the current remediation system. Thus, it is our recommendation to perform some backward particle tracking analysis for the extraction wells.

(11) It appears that there are gaps in capture zones between RWS-7 and its neighboring RWS wells (RWS-6 and RWS-8). The capture zones of these RWS wells remain the focus of this study since these wells are a key component of the remedial system. Backward particle tracking from the screens of these wells may be helpful in identifying the source of the water and contribution of the water from different portions of the aquifer to the RWS wells. This exercise may be also helpful to verify the conceptual model and explain why the hypersaline plume in the deep aquifer is slow to move.

5.2 Suggestions/Recommendations

(1) Further model calibration is recommended with focus on the salt transport. Although the calibration statistics of the current model calibration has showed the model generally matched the water level and salinity at calibration targets, additional calibration with focus on salt transport is recommended. Match of modeled and observed chloride concentration at some TPGW wells need to be improved, especially for the screens at deep aquifer.

(2) There is an urgent need to solve the model calibration problem associated with the model's inability to match the past and current locations of the plume extents. If the model cannot match the existing conditions, any predictions should be interpreted with caution. Development of a set of hydraulically balanced initial conditions (head, mass concentration and temperature) may be a key task for improvement of model predictions. The modeling results from the sensitivity may suggest that an externally generated initial mass concentrations may not work properly with the model.

(3) Backward particle tracking analysis from the RWS wells is recommended, combined with mass balance evaluation, for identification of the sources of water feeding the RWS wells.

(4) Additional sensitivity analyses are suggested for better for better understanding of the hydrogeological dynamics of the system and fate of the hypersaline plume. Additional sensitivity analyses include test of regional gradients, vertical hydraulic connections between the middle and lower high flow zones, effective porosity, etc.

(5) Different additional remediation scenarios, focusing on retracting the plume in the deep aquifer, may be considered and assessed using the model. Only less than five years are left to retract the plume completely to FPL's property to comply with MDC CA, and it might be the time to consider how to enhance the existing RWS so the remediation goals can be met by May 2028. Since it takes time to assess, select, permit, and build an alternative or additional remediation measures, it may be better to consider other options to enhance the remediation. Evaluation of alternative scenarios also provides an opportunity to test, verify, and improve the conceptual model for this model.

1. Introduction

Florida Power and Light (FPL)'s Cooling Canal System (CCS) was constructed in 1973 to provide water for cooling the reactors at its Turkey Point Nuclear Power Plant in Southern Miami-Dade County, Florida. A plume of hypersaline water (chloride concentration exceeding 19,000 mg/l) has formed in the Biscayne aquifer below the CCS due to long term evaporation of the hot water in the CCS (Chin, 2016). The South Florida Water Management District has determined that the plume from the CCS has expanded westward beyond L-31E Canal (SFWMD, 2013).

FPL has reached a consent agreement (CA) with Miami-Dade County (MDC) and FPL (MDC 2015). The MDC CA requires FPL "to demonstrate a statistically valid reduction in the salt mass and volumetric extent of hypersaline water (as represented by chloride concentrations above 19,000 mg/l) in groundwater west and north of FPL's property without creating adverse environmental impacts. A further objective of this Consent Agreement is to reduce the rate of, and, as an ultimate goal, arrest migration of hypersaline groundwater." According to the MDC CA (17.b): FPL shall "intercept, capture, contain and retract hypersaline groundwater (groundwater with a chloride concentration of greater than 19,000 mg/l) to Property boundary to achieve the objectives of this Consent Agreement."

Following the MDC CA, FPL implemented a remediation action plan to retract the plume found west and north of the CCS back to the FPL's property by 2028. As a part of the recovery well system (RWS), 10 groundwater extraction wells were installed along the northern side of the western parameter of the CCS area. These wells are open to the base of the Biscayne aquifer and pump a total of 15 million gallons per day (mgd). Extracted water is collected and discharged into a deep well open to the Boulder Zone (BZ). The remedition system began operating in May 2018.

A variable density groundwater flow and solute transport model was developed by FPL using the USGS SEAWAT code (Guo and Langevin 2003; Langevin et al. 2008) to facilitate proposed remediation options. This model has gone through a number of stages of model calibration and verification. Data from the first four years of operation, including water levels, water quality, Continuous Surface ElectroMagnetic (CSEM) survey data, and monthly salt extration amounts, etc. were used to verify the numerical model and assess the effectiveness of the remediation system.

Groundwater Tek Inc. (GTI) reviewed the 1st year of performance of the RWS and FPL's SEAWAT model (version 3) in 2020 (FPL 2019; GTI 2020), FPL's SEAWAT model version 4 for the CCS salinity eduction application (FPL 2020a), the second year annula report (RAASR Year 2) (FPL 2020b) and associated SEAWAT model version 5 (GTI 2021), and the third year annual report (RAASR Year 3) (FPL 2022) and associated SEAWAT model version 6 (GTI 2022).

The updates to FPL's SEAWAT model in its latest version 7 include: (1) calibration to data (i.e., salinity, water levels, and salt mass extracted) collected from the previous years of operation of the RWS; (2) Increase the vertical resolution by splitting the deep model layers of the prior versions of the SEAWAT models. The updated SEAWAT model now has 17 layers. (3) restructuring the third high flow zone (the lower high flow zone). (4) incorporation of four leakance zones under the cooling canal system (CCS) and (5) Varying the calibration targets and weighting factors.

GTI has been retained and reviewed three of FPL's previous versions of the SEAWAT model (v3 through v6) (GTI 2020; 2021; 2022). This review focuses on the updates and some of technical issues and concerns.

Seven tasks were performed in this review:

(1) Model verification: the calibration and prediction models and sensitivity simulation provided in November 2022 by FPL;

(2) Review of groundwater monitoring data;

(3) Review of salt extraction data and modeling results;

(4) Review of the progress of the hypersaline plume retraction;

(5) Review of sensitivity simulation using the CSEM-based initial salinity conditions;

(6) Review of FPL Remedial Action Annual Report (RAASR) Year 4;

(7) Review of SEAWAT model version 6: the updates and model recalibration.

This technical report summaries the review of the data, report and models, discussion, and comments. Suggestions and recommendations are provided for future model development.

2. Model Verifications

FPL provided the model input and output files of the SEAWAT models:

- The calibration models;
- The base-prediction model;
- The sensitivity simulation model using the initial salinity condition based on the 2022 CSEM survey data and modeling data;
- The sensitivity simulation model considering L-31E Canal as a drain.

As a step of verification, all of these models were rerun independently using the information and files provided by FPL. The outputs from these models were compared to the report and output files from FPL to validate the inputs and outputs.

2.1 Verification of Calibration Models

The model calibration includes a series of models for different time periods:

- Pre-development steady-state flow-only model (Prior to 1940);
- Steady-state flow and transient transport calibration model (1940 – 1968);
- Seasonal transient flow and transport calibration model (1969 – 2010);
- Monthly transient flow and transport calibration model (2010-2022).

The steady-state model, the seasonal model and the monthly model use the results (heads, salinity, and temperature) from previous models as the initial conditions. FPL provided a Windows Batch file to facilitate the execution of these models.

The final output files contain the results (simulated heads, salinity, and temperature) of 140 monthly stress periods from 2010 to 2022, including 4 years of RWS operation.

2.2 Verification of The Prediction Models

The prediction model used the results from the end of monthly calibration model (May 2022) as the initial conditions for salinity, heads and temperature. This model has 72 monthly stress periods, covering a time period from June 2022 to May 2028. The time-dependent boundary conditions were based on inputs from 2018 to 2022 in the last four years of model calibration. And the data were repeated 1.5 times in the prediction simulations.

The verification run of the prediction model was completed successfully.

2.3 Verification of The Sensitivity Analysis Runs

Two sensitivity analysis simulations were performed by FPL, based on the prediction model. In one sensitivity run, the L-31E Canal was modeled using MODLFOW DRAIN package rather than the RIVER package in the calibration and prediction models. The sensitivity analysis was designed to investigate the impact of the canal to the transport of hypersaline water.

In the second sensitivity analysis run, the predictive timeframe was modeled starting with an initial salinity condition based on a combination of CSEM and modeled data. This run was designed to investigate if the initial salinity condition inherited from the calibration model would cause the model to be unable to predict the hypersaline plume retraction in the deep Biscayne aquifer.

When the supplied windows batch file “Predict_V7.bat” was executed, the errors for missing input files appeared:

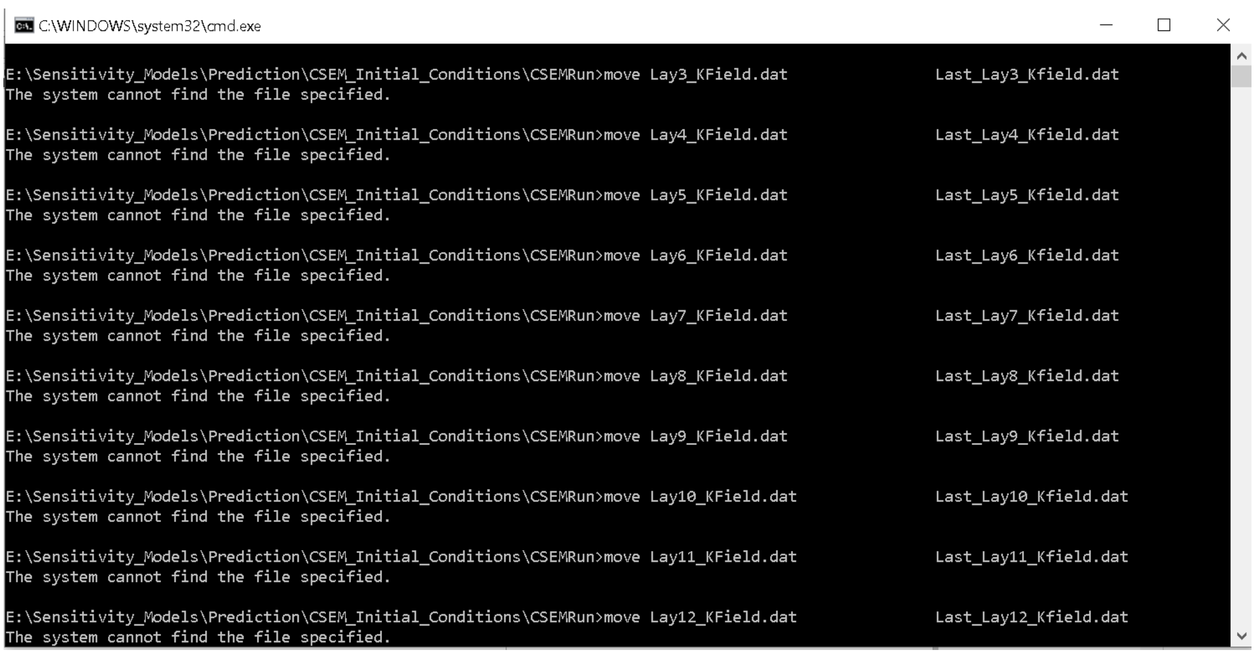

Similar input files were found in the folder for another sensitivity analysis run for L-31E Canal. It is not clear if these files found in the other folder are the same as the ones to be used in the CSEM-initial salinity condition sensitivity run. In an attempt to test whether the sensitivity run would execute, these similar files were copied and used for this sensitivity run. With these “borrowed” input files, the batch commands continued but soon another error message for missing input files appeared as follows:

```
Program PPK2FAC calculates point-to-cell factors by which kriging is
  undertaken from a set of pilot points to the finite-difference grid.

Enter name of grid specification file:   - grid specifications read from file FPL_v7_Grid.spc
Enter name of pilot points file:  Error: cannot open pilot points file Kh_v7.dat - try again.
Enter name of pilot points file:  Error: cannot open pilot points file 0.1 - try again.
Enter name of pilot points file:
Errors in pilot points file .\PilotPoints\Zone_KhL3.inf ----->
  Line 28: insufficient entries (five entries required).
  Line 56: insufficient entries (five entries required).
  Line 84: insufficient entries (five entries required).
  Line 112: insufficient entries (five entries required).
  Line 140: insufficient entries (five entries required).
  Line 168: insufficient entries (five entries required).
  Line 196: insufficient entries (five entries required).
  Line 224: insufficient entries (five entries required).
  Line 252: insufficient entries (five entries required).
  Line 280: insufficient entries (five entries required).
  Line 308: insufficient entries (five entries required).
  Line 336: insufficient entries (five entries required).
```

It appeared that two input files were required for continuous execution of the batch file. The entire folder was searched to see if similar files can be found. A file with the same name "kh_v7.dat" was found but the file name "0.1" was not found.

2.4 Verification of Monthly RWS Pumping and Salt Extraction Rates

The chart below (**Figure 2-3)** shows the monthly total pumping rates (in million gallons per day or mgd) and monthly totals of salt extraction (million pounds) from the RWS recovery wells tapping the bottom of the Biscayne Aquifer represented.

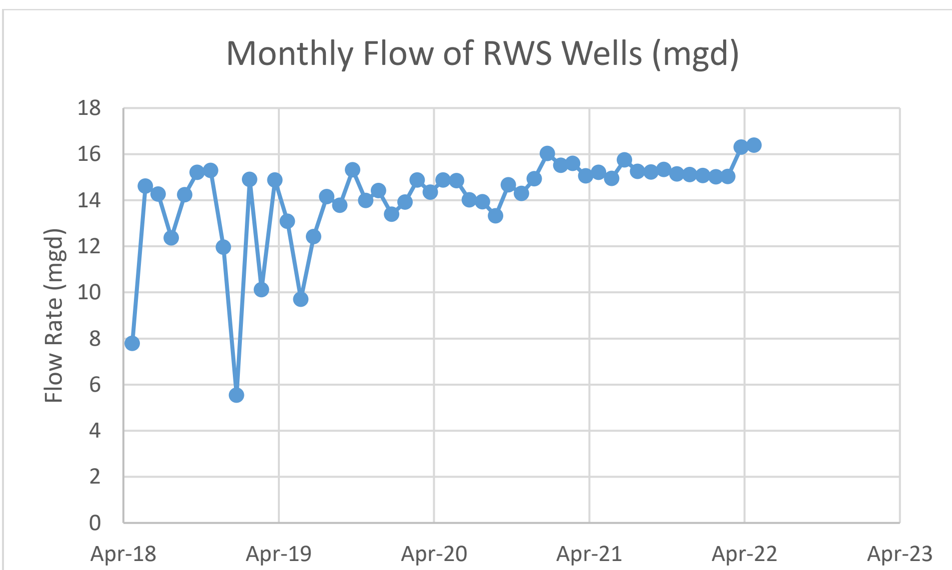

Figure 2-3: Total pumping rates of the RWS wells (mgd).

The amounts of monthly salt extraction from the RWS wells are shown in **Figure 2-4**. The published values, as weekly data reported in the RAASR Yr 4, are also shown in Figure 2-4 for comparison. The reported monthly salt extraction shown in Figure 2.4 are estimated from the figure in the FPL's RAASR Yr 4 (FPL 2022: Figure 5,.3-5). The amount of salt extracted per month from 2018 to 2022 appears to be quite stable in the ranges between 150 to 180 million pounds per month.

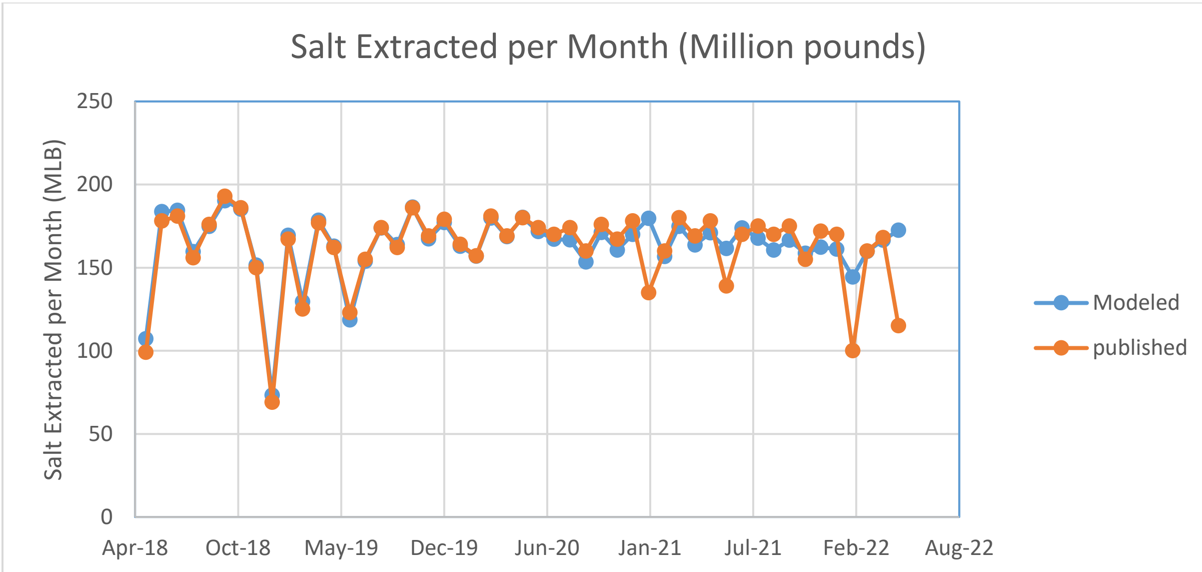

Figure 2-4: Comparison of Monthly total of salt extraction from the RWS wells.

Figure 2-5 shows the monthly sat extraction rates reported by FPL (2022). The comparison between the results, modeled salt extraction rates, based on GTI's verification runs of the monthly calibration SEAWAT model, appears that the modeled salt extraction rates from FPL and GTI are in close agreement with published data.

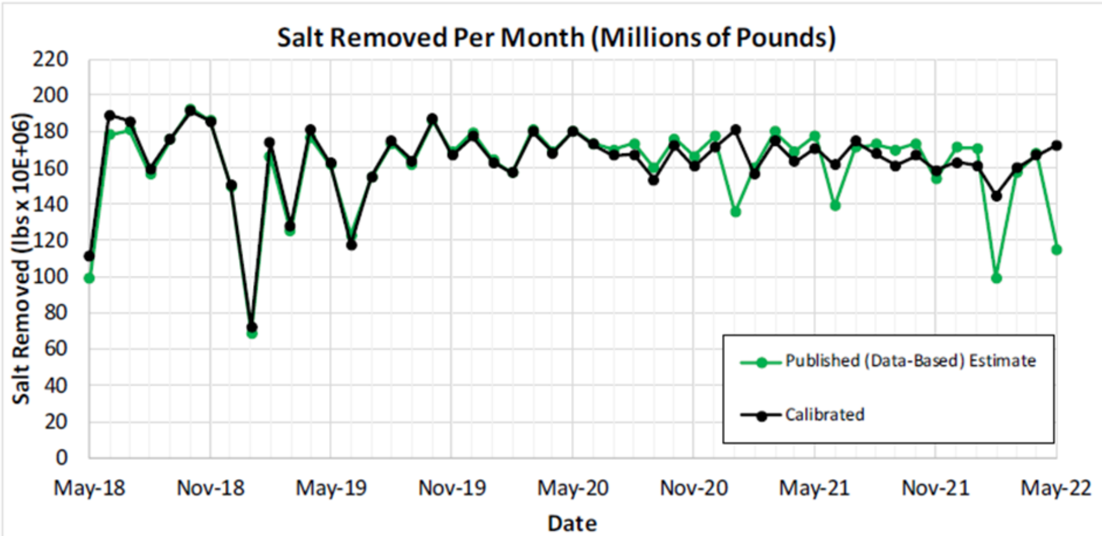

Figure 5.2-4. Comparison of Model and Observed Total Mass Extracted by the RWS Between May 2018 and May 2022

Figure 2-5 shows the monthly salt extracted salt, modeled by FPL and published values.

2.5 Verification of Plume Retraction Prediction

Figure 2-6 shows the comparisons of model-predicted hypersaline plume extents after 5 and 10 years of remediation operation (from 2018 to 2028) in model layers 4, 9, 13, and 16, respectively. These four layers represent the shallow, middle, and upper and lower deep high flow zones of the Biscayne Aquifer. In each of these four figures, the model-predicted plume extents shown by FPL (FPL 2022: Figures 5.3-1a through 5.3-1d) are compared side-by-side with the results based on the verificative rerun of the base-prediction model in this review (labeled as GTI). The comparison indicates the modeling results reported by FPL can be successfully and independently reproduced.

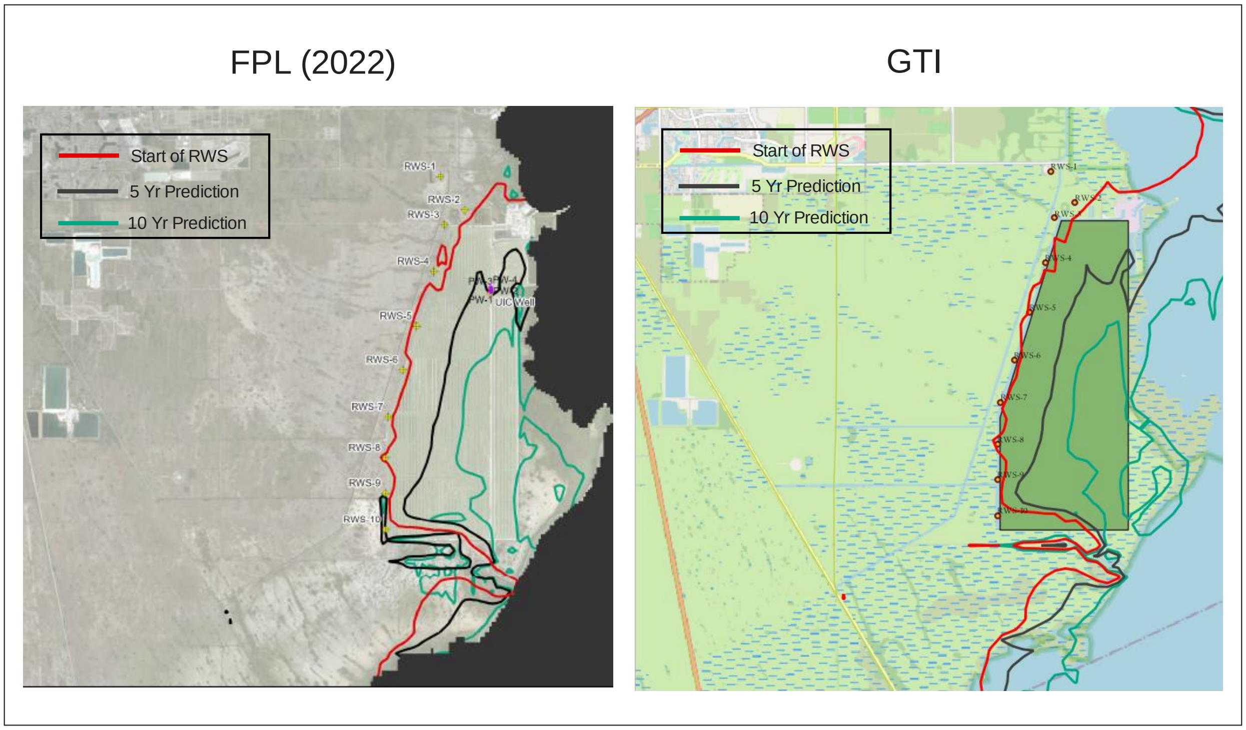

(a) Model Layer 4 (The Shallow High Flow Zone)

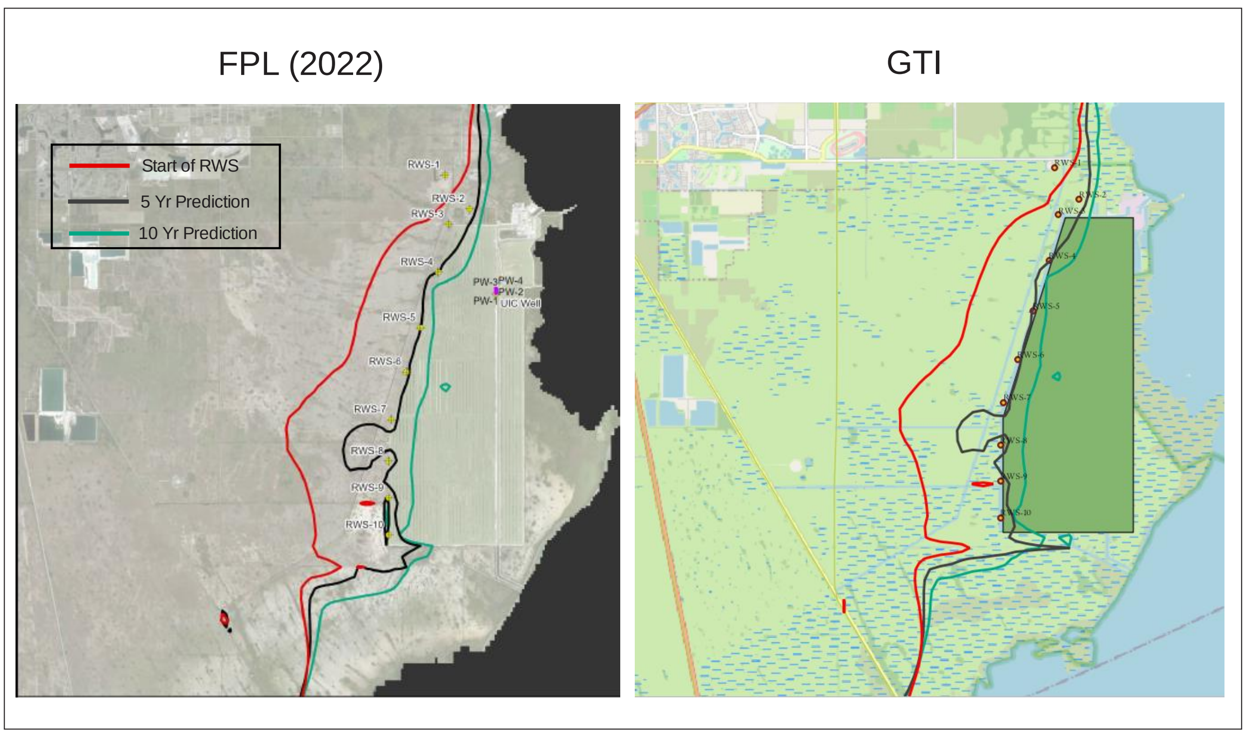

(b) Model Layer 9 (The Middle High Flow Zone)

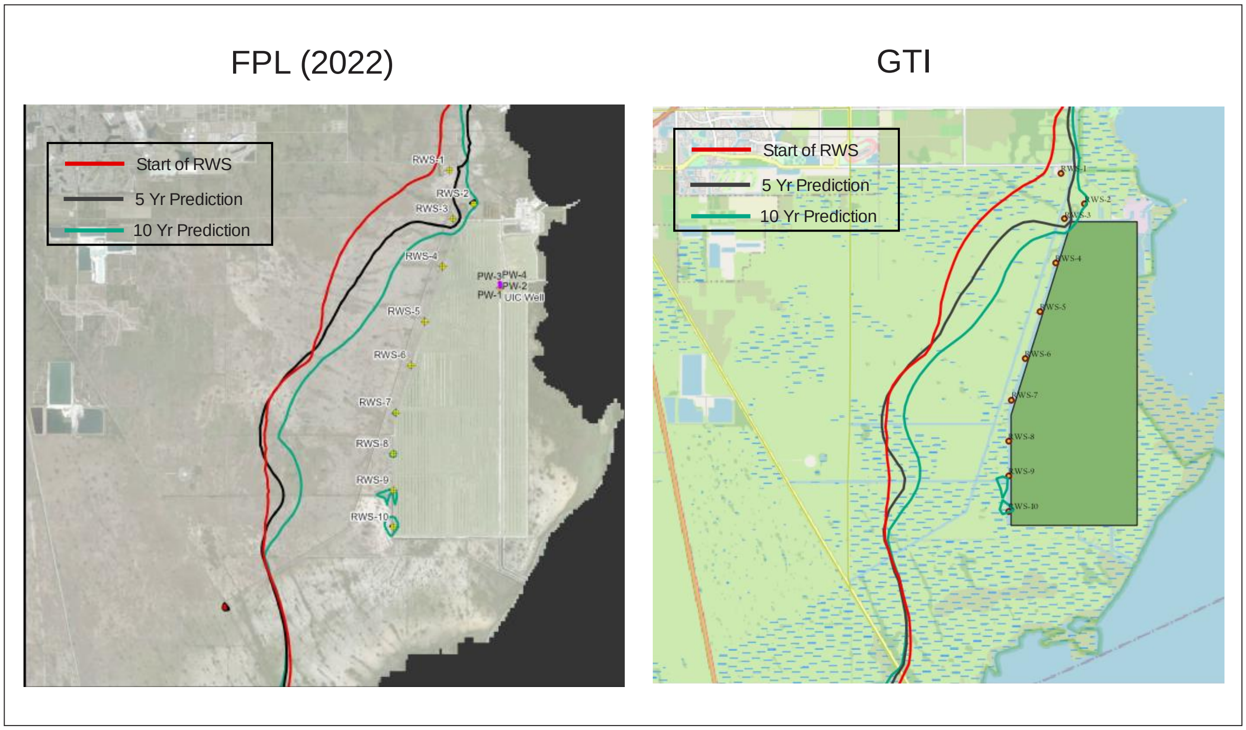

(c) Model Layer 13 (The Upper Deep High Flow Zone)

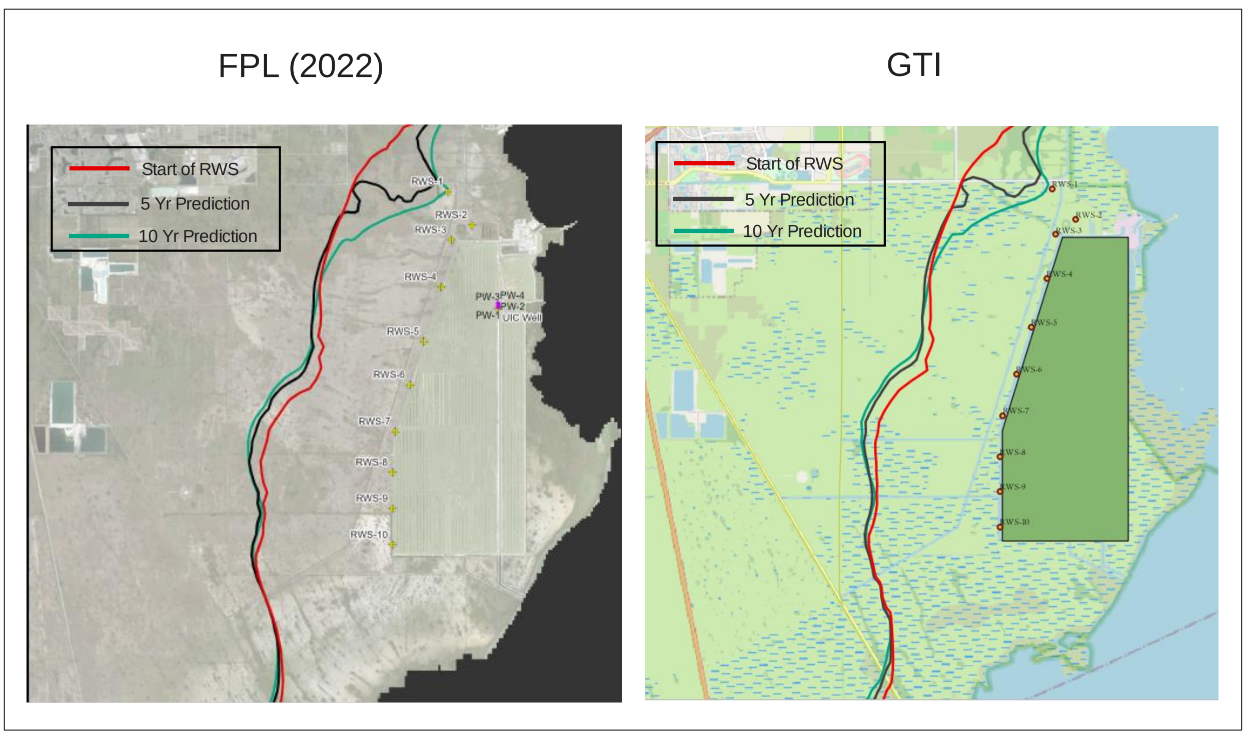

(d) Model Layer 16 (the Lower Deep Flow Zone)

Figure 2-6: Comparisons of the extents of the hypersaline plume at selected model layers.

Note that FPL's prediction shows the plume extent in the lower deep high flow zone (Figure 2-6(d)) has slightly expanded westward from its initial location when the RWS started operation in 2018. This plume move direction is contradictory to the conceptual model. And as shown in the figure, most of the westward expansion occurred in the first five years of remediation. This western migration in the deep aquifer is expected to slow down after 2023, then the plume will essentially become stagnant. This confirms what FPL noted that "Due west of the southern portion of the CCS in layers 16 and 17, however, the plume is shown to expand further west through year 5 and halts or slows by Year 10 of remediation." (FPL 2022: p. 5-22). And FPL suggested "This forecast is contrary to Year 4 CSEM survey results that show net retractions of the plume exceeding 60% along the base of the aquifer has already occurred from 2018 through 2022 as shown on Table 4.3-1 and visually in Appendix G 6A." (FPL 2022: *Figures 5.3-1 a, b, c, d*).

3. Review of Sensitivity Simulations (CSEM Data-Based Initial Salinity Condition)

3.1 Initial salinity based on the CSEM data (SA1):

One of the major concerns regarding the FPL's SEAWAT model is its inability to match the extents of the hypersaline plume in the deep Biscayne aquifer (GTI 2020; 2021; 2022). The model-predicted plume retraction showed little changes in deep model layers 13 and 16 after 10 years of remediation (as shown in Figure 2-6(c) and (d) in the previous section). FPL has argued that CSEM survey data has actually shown retraction in the deep Biscayne aquifer but the model simulation results didn't appear to show significant retraction of the plume but even slightly westward expansion of the plume from 2018 to 2023 (5 year of the RWS operation).

To test whether a set of initial CSEM-based salinity conditions may improve the model's prediction, FPL performed a sensitivity analysis simulation using a set of initial salinity conditions by combining the2022 CSEM survey data and modeling data. The results are compared to the base run, which used the initial conditions derived directly from the last stress period (May 2022) of the model calibration simulation.

Model-predicted plume extents in 2023 (Yr 5) and 2028 (Yr 10) using different initial mass concentration in selected model layers are shown in **Figure 3-1**. The solid lines represent the results based on model-calibrated initial conditions (i.e. the concentration from the last stress period of the calibration model corresponding to May 2022) and dashed lines represent the results based on the CSEM survey data and modeling data. It appears the results are not significantly different using either the calibrated salinity or mixed CSEM and modeling data for shallow and middle layers (Figure 3-1(1) and (2)). However, model-predicted plume extents are quite different when CSEM-based initial mass concentration conditions were applied for deeper layers (Figure 3-1(3) and (4)). The simulation with CSEM-based initial mass concentration condition would show the plume extents closer to the CCS, but the displacement of the plume extents from 2023 to 2028 is still relatively small.

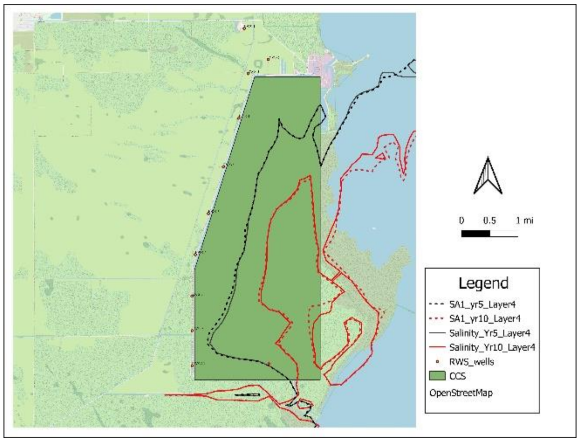

(1)

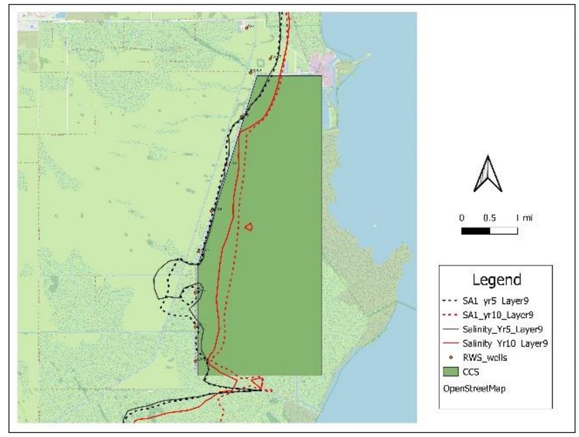

(2)

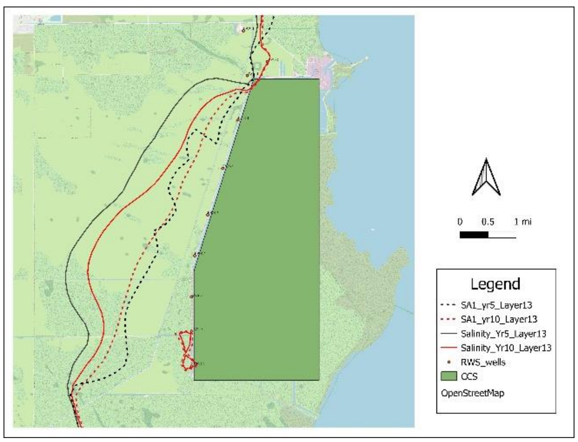

(3)

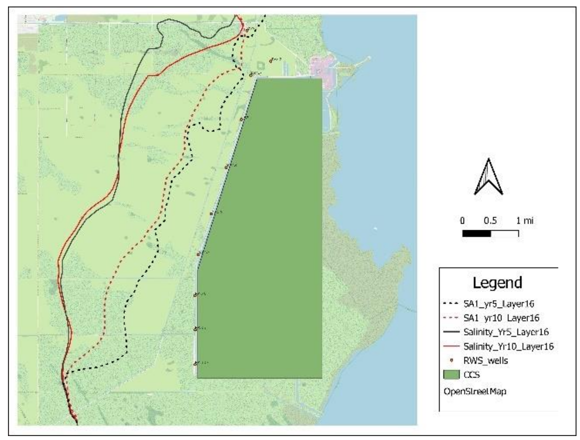

(4)

Figure 3-1. Comparison of 5 and 10 years of model predictions from the Base-run and SA1 in model (a) Layer 4, (b) Layer 9, (c) Layer 13 and Layer 16.

Comparisons of modeled plume extents after 5 years (or May 2023) and 10 years (or May 2028) in model layer 16 are shown in **Figure 3-2**. The results of the simulation indicate the locations of plume extents do not change significantly in the shallow and middle layers when initial salinity conditions based on CSEM data were applied, compared with the base run conditions. However, the model-predicted the plume extent in deep model layers after 10 years of RWS actually moved westward from that after 5 years (e.g. Layer 16 as shown in Figure 3-2) from the initial location.

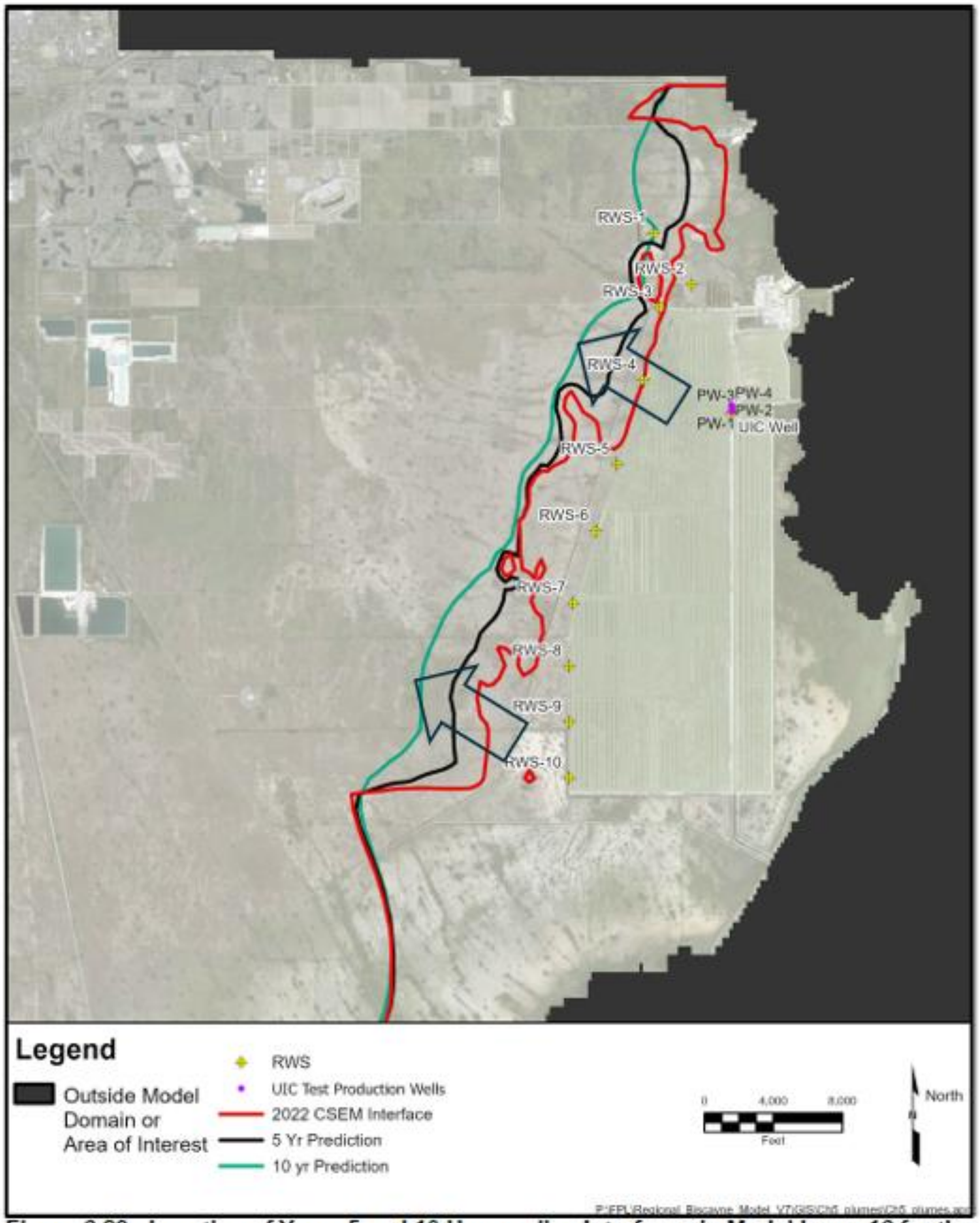

Figure 6-29. Location of Years 5 and 10 Hypersaline Interfaces in Model Layer 16 for the First Sensitivity Simulation.

Figure 3.2 Location of the plume extent after Yrs 5 (2023) and 10 (2028) in Model Layer 16 (SA1). The arrows indicate the move direction of the hypersaline plume extent.

FPL (2022) concluded "The results of this simulation are similar to the base model simulation in the upper 11 layers. However, consistent with the original model, the movement of the interface in layers 13 and 16 (FPL 2022: Figures 6.28 and 6.29) shows mixed results with westward movement in some areas during the 10-year remediation period." And FPL (2022) concluded “The interface continues westward movement under the influence of hydraulic and density gradients when outside the capture zone. This simulation suggests that the model’s inability to align interface movement with the CSEM data is related to the representation of the near-RWS flow system.” This review agrees with FPL’s conclusion.

One of the possible reasons for the disparity between the modeling results and CSEM surveys may be the unmatched initial salinity distribution in the model (GTI 2021; 2022). In FPL’s SEAWAT models, the initial heads, salinity, and temperature data for the prediction models all were derived from the end of the model calibration periods. This set of model-derived initial salinity conditions may not be consistent with the actual salinity distribution that should be hydrodynamically equilibrated with the groundwater flow regime. Therefore, unbalanced positions of the initial plume as of May 2018 would likely impact the salt transport simulation and lead to unrealistic model predictions.

Based on the results of this sensitivity analysis, we can also conclude that a set of externally generated initial salinity conditions, like the one used in this sensitivity simulation, may not work well because externally generated initial salinity conditions may not hydrodynamically equilibrated with the head distribution in the model. For a solute transport simulation, the model may take time to adjust the system to balance with the initial salinity conditions (as loadings to the model). The time for the adjustment could be long.

From this sensitivity analysis simulation, we may also conclude that it may be necessary to focus the model calibration to the starting time of the RWS system (i.e. April 2018). If we are not able to match the plume before RWS operation, it will be difficult to correctly calibrate the model to match the salinity distribution in May 2022 and use the model for future prediction, when we consider the movement time for the plume.

3.2. L-31E Canal as A Drain (SA2)

The L-31E Canal is modeled using MODFLOW River package, which allows for water exchange between the canal and the aquifer, depending on the water levels. When the stage inside the canal is higher than the water levels outside, water flows from the canal to the aquifer, and some of the water may be withdrawn by the RWS wells.

This sensitivity analysis simulation (SA2) was designed to evaluate the impact of the L-31E canal, as a potential source of water, to the remedial efficiency of the RWS wells. The canal was modeled using MODLFOW Drain package in this sensitivity analysis, which allows only water to flow into the canal when the aquifer water levels are higher than the canal stage. As indicated by FPL (2022), by eliminating this drainage canal as a source of freshwater to the aquifer, the RWS wells must source their extracted water from a within the aquifer, as opposed to pulling water from the L-31E canal. Without water from the canal, a greater remedial efficiency in terms of hypersaline plume removal and greater hypersaline may be expected.

Comparisons of modeled plume extents after 5 years (or May 2023) and 10 years (or May 2028) in model layers 4, 9, 13, and 16 are shown in **Figure 3-3**.

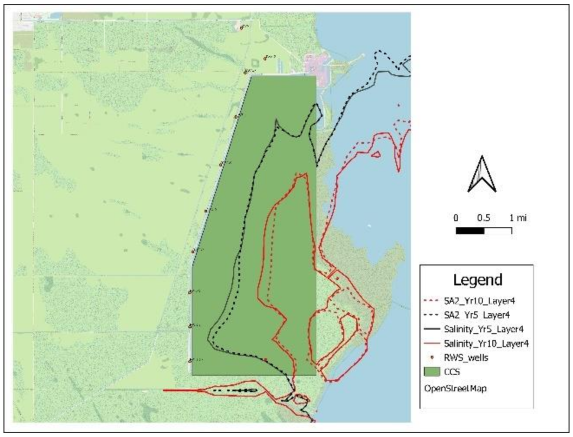

(1)

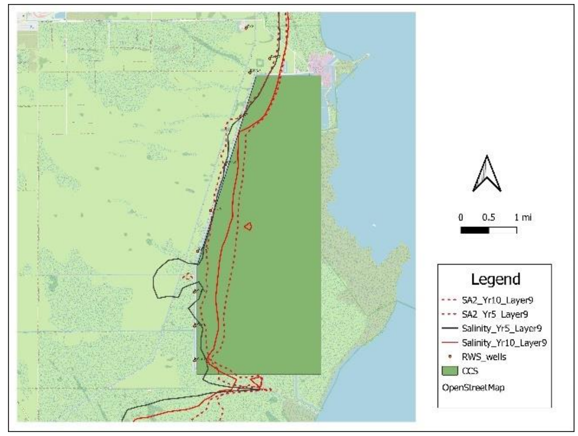

(2)

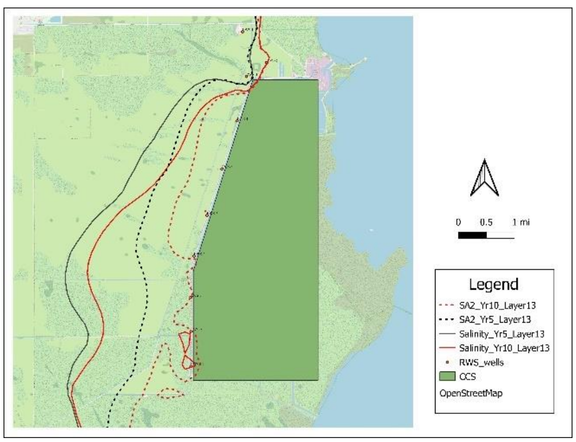

(3)

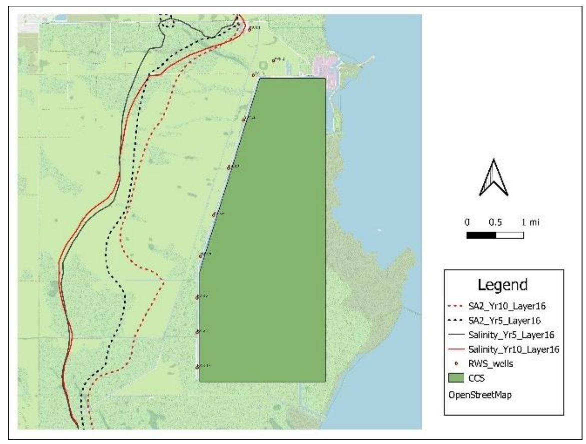

(4)

Figure 3-3. Comparison of 5 and 10 years of model predictions from the Base-run and SA2 in model (a) Layer 4, (b) Layer 9, (c) Layer 13 and Layer 16.

The results shown in Figure 3-3 indicate the plume retraction are not significantly different for the shallow and middle portions of the aquifer as shown in Figures 3-3(1) and (2) when the L-31E Canal was modeled as a drainage feature. However, in the upper portion of the deep high flow zone (model layer 13), the hypersaline plume was significantly retracted towards the CCS, as shown In Figure 3-3(3). This suggests that remedial efficiency of the RWS wells may be sensitive to the availability of water from the shallow layers above. However, the impact to the hypersaline plume is weaker at deeper depth such as model layer 16 (as shown in Figure 3-3(4).

4. Review Comments of FPL's RAASR Year 4 and SEAWAT Model v7

The comments presented below were based on the review of the 4th year of RAASR report (FPL 2022) and FPL's variable density groundwater flow and solute transport SEAWAT model (v7).

(1) The RWS System

FPL concluded that "Data and modeling confirm that the objectives of the MDC CA and FDEP CO through Year 4 have been met." (ES p.2). This review agrees with FPL's this conclusion in general. FPL used three primary tools to assess remediation progress: groundwater monitoring data, continuous surface electromagnetic (CSEM) survey, and groundwater modeling.

The groundwater monitoring data over the four-year time period have indicated a general downward trend of salinity in the Biscayne Aquifer in the study area, especially in the shallow and middle flow zones of the Biscayne aquifer.

The groundwater recovery wells system (RWS) appears to function as expected. Approximately 23.43 billion gallons of hypersaline groundwater water and 9.24 billion pounds of salt have been extracted. Approximately 6.18 billion gallons of hypersaline water and 2.37 billion pounds of salt were removed in this time period (from June 2021 to May 2022).

Both the CSEM survey data and groundwater modeling results have showed the westward expansion of the hypersaline plume originated from the CCS has been halted in most parts of the compliance area. The hypersaline plume has been retracted towards the CCS in the top two thirds of the Biscayne aquifer.

(2) Change of layers

The major change of FPL SEAWAT model version 7 from previous versions is the increase of vertical resolution by splitting the deeper model layers. The current model has 17 layers, increased from 11 layers in previous models. A comparison of the previous and current model layers is shown in **Table 4-1**.

The deep high flow zone in the previous models is split to the upper portion and the lower portion. Figure 4-1 (FPL 2022) shows the middle and deep model layers and a cross-sectional view of the middle high flow zone (MHFZ) and the low high flow zone (LHFZ). The increase of model layers helps more accurately locate the screens of monitoring wells and extraction wells.

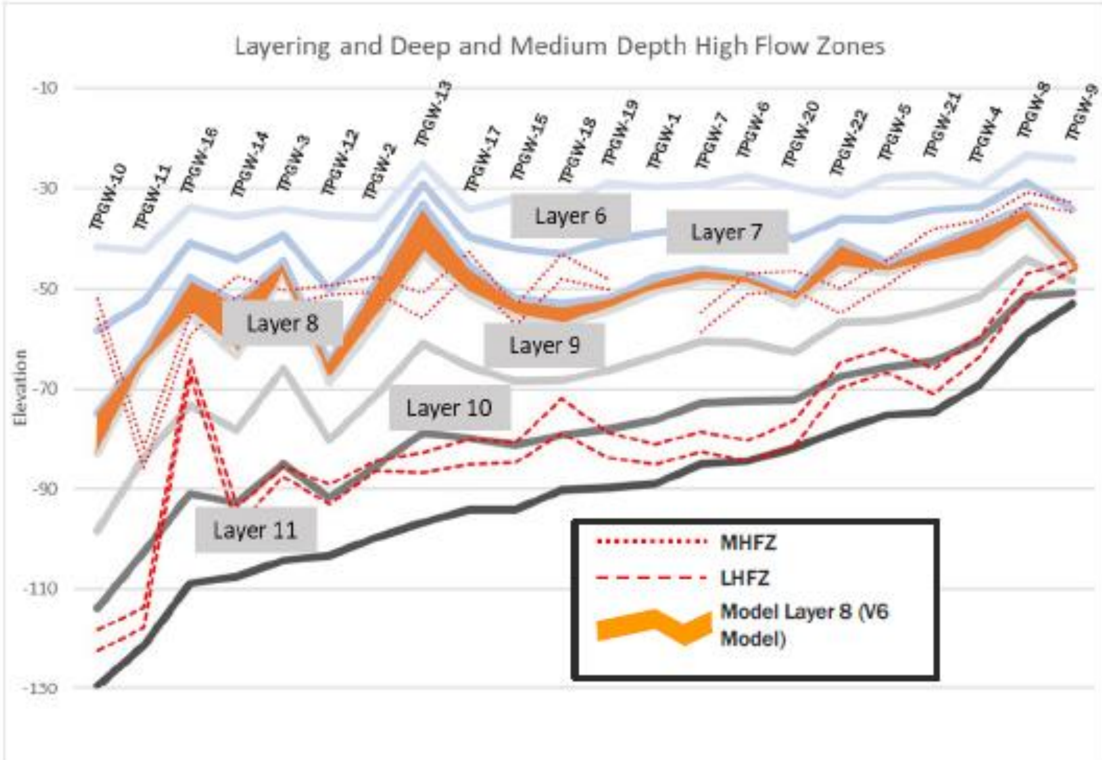

Figure 4-1. Representation of V6 model layer elevations and the elevations of the MHFZ and LHFZ at TPGW well locations.

Prior Models	**Model V7**
Layers 1-6	No change
Layer 7	7, 8
Layer 8	9
Layer 9	10, 11
Layer 10	12, 13, 14
Layer 11	15, 16, 17

Table 4-1. Model layer Changes from the prior models to v7.

Figure 4-2 shows the comparisons of simulated plume extents at year 10 (2028) in selected model layers based on the previous version (v6) and current version (v7) of the FPL SEAWAT model. The increase of the model layers does not appear to change the overall picture of the model simulations. The most prominent difference appears to be at TPGW-1 in model layer 13 (Layer 10 in previous models), as shown in Figure 4-2(3), where simulated plume extent is much closer to the L-31E Canal based on the current version of SEAWAT model. It should note that the difference at TPGW-1 may not be necessarily caused by the increase of model layers.

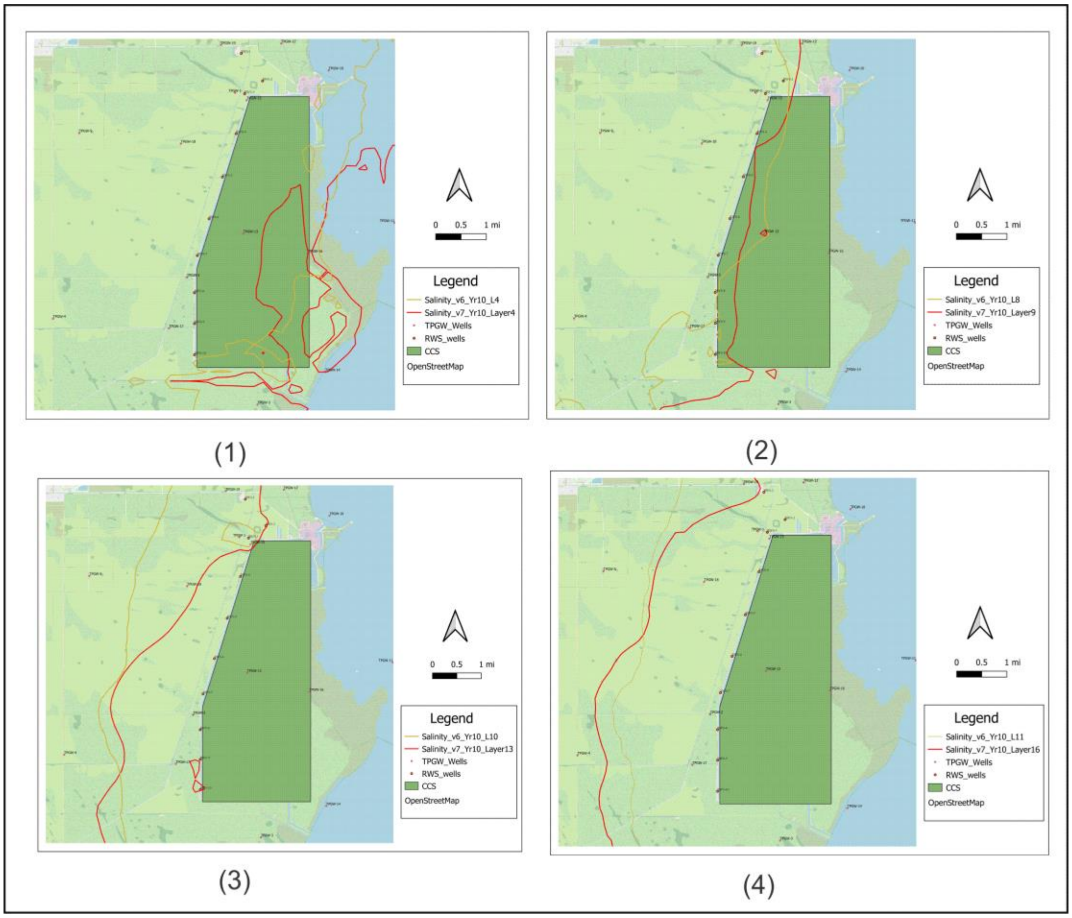

Figure 4-2. Comparison of simulated plume extents at year 10 (2028) in selected model layers based on FPL SEAWAT v6 and v7.

(3) Model calibration

The model presented in this report is the seventh generation of the variable density groundwater flow and salt transport SEAWAT model. In general, the current version of the SEAWAT model is well developed with good modeling practices. The model has been gone through a number of rigorous model calibration steps. Based on the calibration statistical summary for the version 7 model presented **Table 5.2-1** (FPL 2022: p. 5-12), it appears that the model has been reasonably well calibrated to the calibration targets. The model predicted water levels, monthly salt extraction rates, and salinity in most of monitoring wells as well as the CSEM survey data.

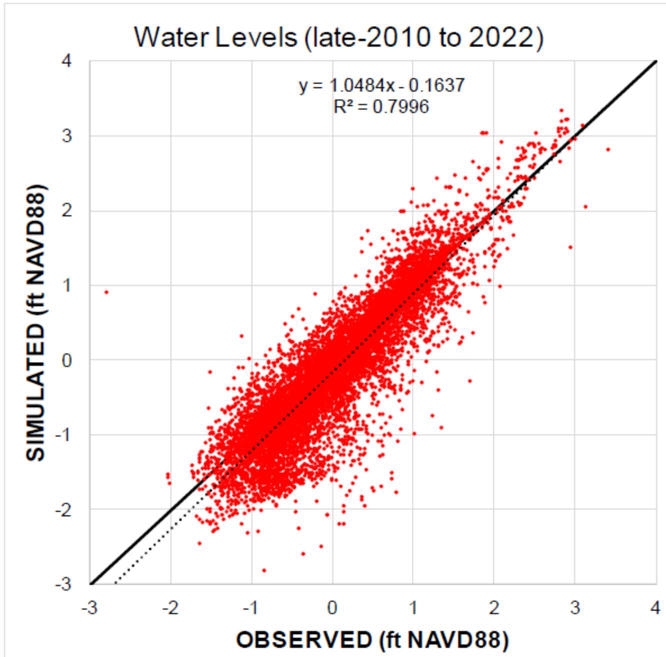

Figure 5-7. Plot of observed versus simulated water levels (ft NAVD88) for the monthly model.

Figure 4-3. Plots of modeled and observed water levels (ft, NAVD 88) (FPL 2022).

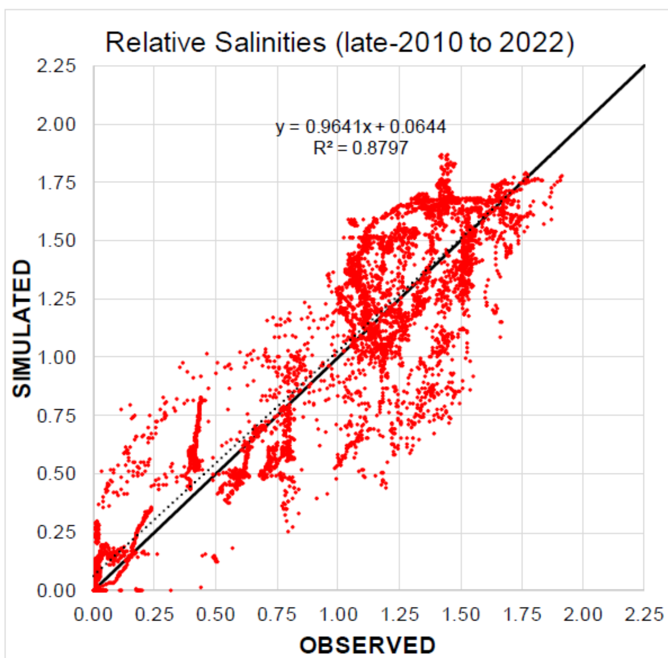

Figure 5-8. Plot of observed versus simulated relative salinity for the monthly model.

Figure 4-4. Plots of modeled and observed relative salinity (FPL 2022).

The figures (**Figures 4-3 and 4-4**) above are often used to demonstrate the correlation of model computed and observed values at observation locations. Ideally, all points should fall on a 45 degree line, indicating a perfect match. However, the points are often falling off the line as model calibrations are never perfect.

The points shown on these two figures indicate the calibrated model is in close agreement with observed data at the observation locations.

It appears that head calibration is relatively more consistent than the relative salinity, but statistically the R^2 for salinity (R^2=0.88) is slightly better than that for heads (R^2=0.8).

Based on the charts showing calibrated and measured salinity (FPL 2022: Appendix I: Figure 5-10), it appears that the differences between observed and modeled salinity are still large at some of the TPGW monitoring wells, and the solute transport calibration needs to be improved in the future.

Table 4-2: Model calibration statistics (FPL 2022).

Ta alibration Statistic Summary for the V7 Model

Model	Target Type	Units	ME	MAE	RMSE	MAE ÷ Range
Seasonal (1968-2010)	Hydraulic Head	ft	-0.130	0.464	0.614	6.8%
	Relative Salinity	R.S.	0.013	0.090	0.163	5.4%
Monthly (2010-2022)	Hydraulic Head	ft	-0.162	0.325	0.447	5.2%
	Relative Salinity	R.S.	0.034	0.161	0.216	8.4%
CSEM (2018 through 2022)	2018 CSEM Survey	R.S.	0.017	0.230	0.313	11.2%
	2019 CSEM Survey	R.S.	0.066	0.252	0.343	12.2%
	2020 CSEM Survey	R.S.	0.086	0.241	0.332	11.7%
	2021 CSEM Survey	R.S.	0.091	0.229	0.319	11.2%
	2022 CSEM Survey	R.S.	0.142	0.245	0.346	11.9%

Note: One Relative Salinity (R.S.) Unit = 35 PSU = 19,400 mg/L Cl

It should be noted that a close agreement between modeled and observed values at observation targets is necessary, but it is not sufficient for a well calibrated model. As discussed above, some model calibration issues remain and need to be identified and fixed.

Although the calibration statistics shown in **Table 4-2** suggest the model has been reasonably well calibrated to the targets, the modeled plume extents are still significantly different from those delineated by the CSEM survey data. The explanation for this paradox may be related to the distribution of the calibration targets. Perfect matches to the calibration targets do not necessarily guarantee the model will make perfect predictions. It also depends on the spatial and temporal distributions of the calibration targets. Lack of monitoring salinity data in the deep Biscayne Aquifer may contribute to the disparity. One recommendation is to compute the calibration statistics for each flow zone so we can get a better picture of the model calibration.

(4) Match of the Deep Model Layers

Figure 4-3 and 4-4 show the typical plots of modeled versus observed water levels and relative salinity as a quality check of model calibration. It would be interesting to compare the distributions of simulated and observed relative salinity by mode layers. Due to the limited availability of monitoring wells, the salinity derived from the CSEM survey data is used for the comparison.

FPL prepared a sensitivity analysis simulation using CSEM-derived initial salinity conditions for model prediction. The initial CSEM-derived salinity can be assumed to be representative of the relative salinity in May 2022. Since the last stress period of calibration model is also May 2022, we can compare simulated salinity from the end of model calibration run to the initial salinity data for the SA1 as a quality check of model calibration.

Typically, the initial mass concentration is contained in the BTN (one of the MT3DMS input files). However, the relevant BTN is not found in the file folder. It is likely missing because the verification run of this sensitivity analysis simulation was unsuccessful as discussed in Section 2 of this report. To make the comparison possible, the initial CSEM-derived salinity data was extracted from a file called "Belended_v7_iniSalt.dat" in the file folder:

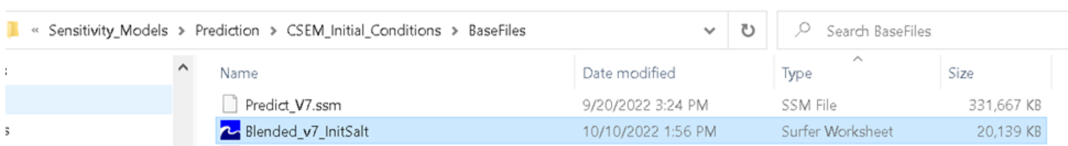

The raw data extracted from Blended_v7_iniSalt.dat were kriged using Golden Software Surfer and exported as GIS shapefiles for selected model layers 4, 9, 13 and 16. The comparison is plotted for these selected layers and shown in **Figure 4-5**.

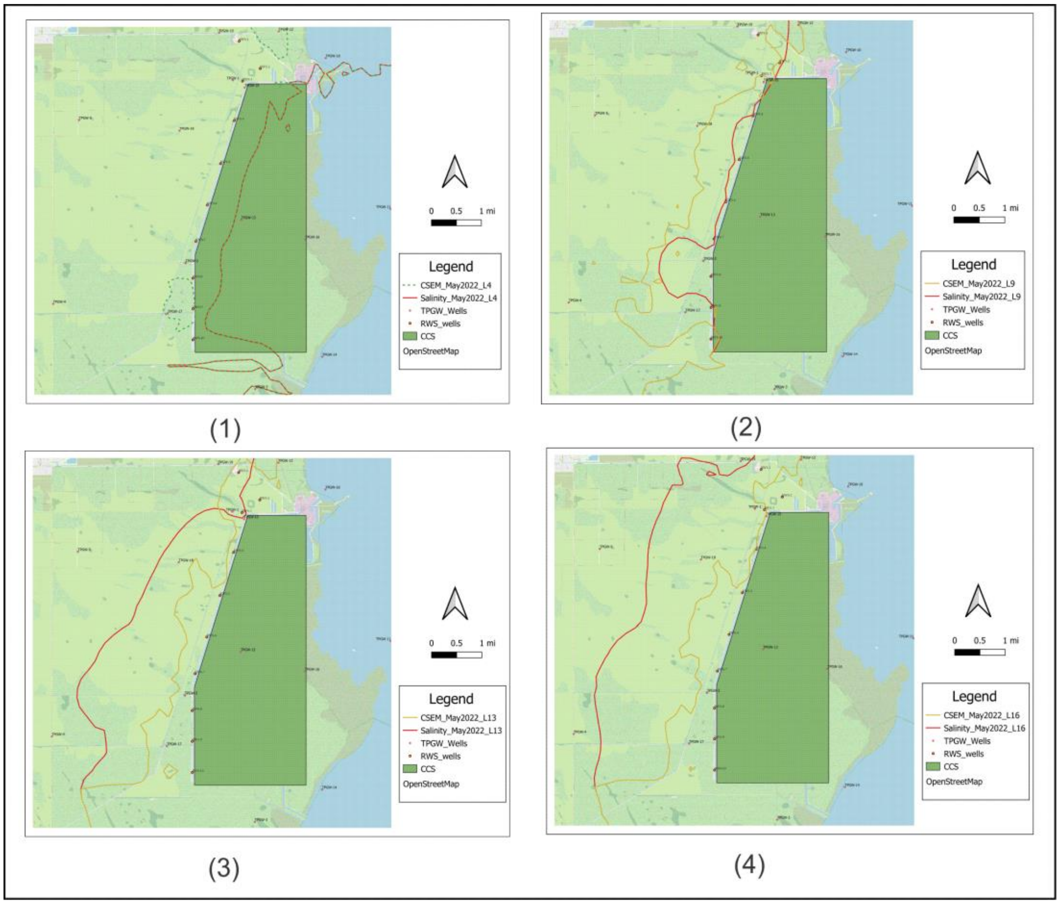

Figure 4-5. Comparison of simulated relative salinity and CSEM-converted relative salinity in selected modeled layers for May 2022.

As shown in Figure 4-5: the salinity match in Layer 4 is perfect. This may be because the CSEM data was used only for deep layers while the modeled data were used for the shallow layers. The CSEM-derived plume extent is behind simulated plume extent (Figure 4-5(2)) while the CSEM-derived plume extent is much closer to L-31E canal in model layers 13 and 16 (Figure 4-5 (3) and (4)). These two layers represent the deep portion of the Biscayne aquifer. Therefore, if we assume CSEM-derived salinity data are representative of real salinity in the aquifer, then the model is unable to match field conditions for the deep portion of the aquifer.

(5) Model Predictions

In general, the major applications of groundwater models fall into two categories: scenario comparison and future prediction. FPL has used the earlier version of this SEAWAT model to select the existing RWS system by comparing a number of remediation scenarios and selected the current remediation design in 2015.

The model's inability to match the plume extents in the deep layers, representing the deep portion of the Biscayne aquifer, remains a major concern. Among the three primary tools that FPL used to assess the remediation progress, groundwater modeling is probably the only predictive tool that may provide timely assessment of whether or not the MDC CA and FDEP CO's remediation objectives will be met. Identification of the problems and further model calibration with focus on the historic match of plume extent are critical and urgent in future model development.

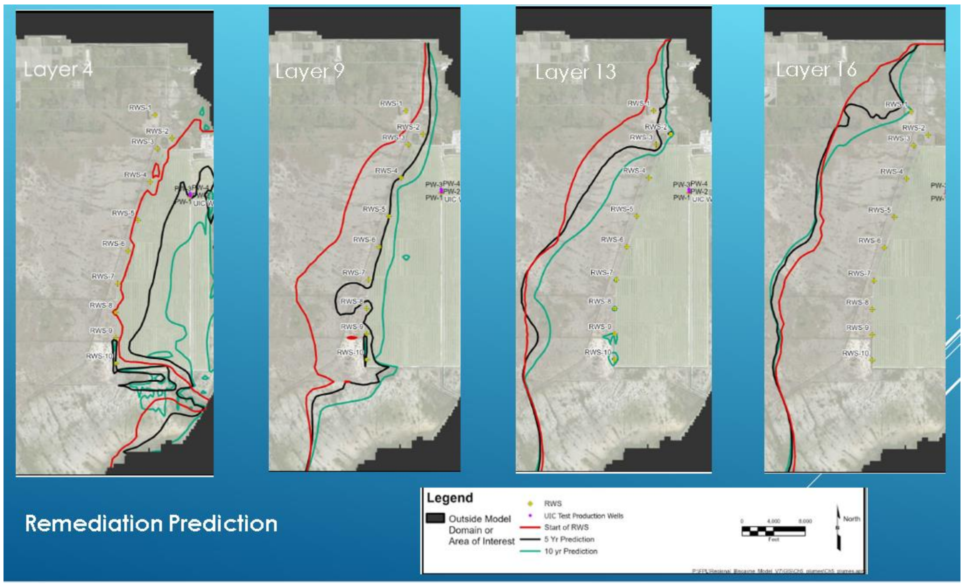

Figure 4-6. Model-predicted plume extents in selected model layers (FPL 2022).

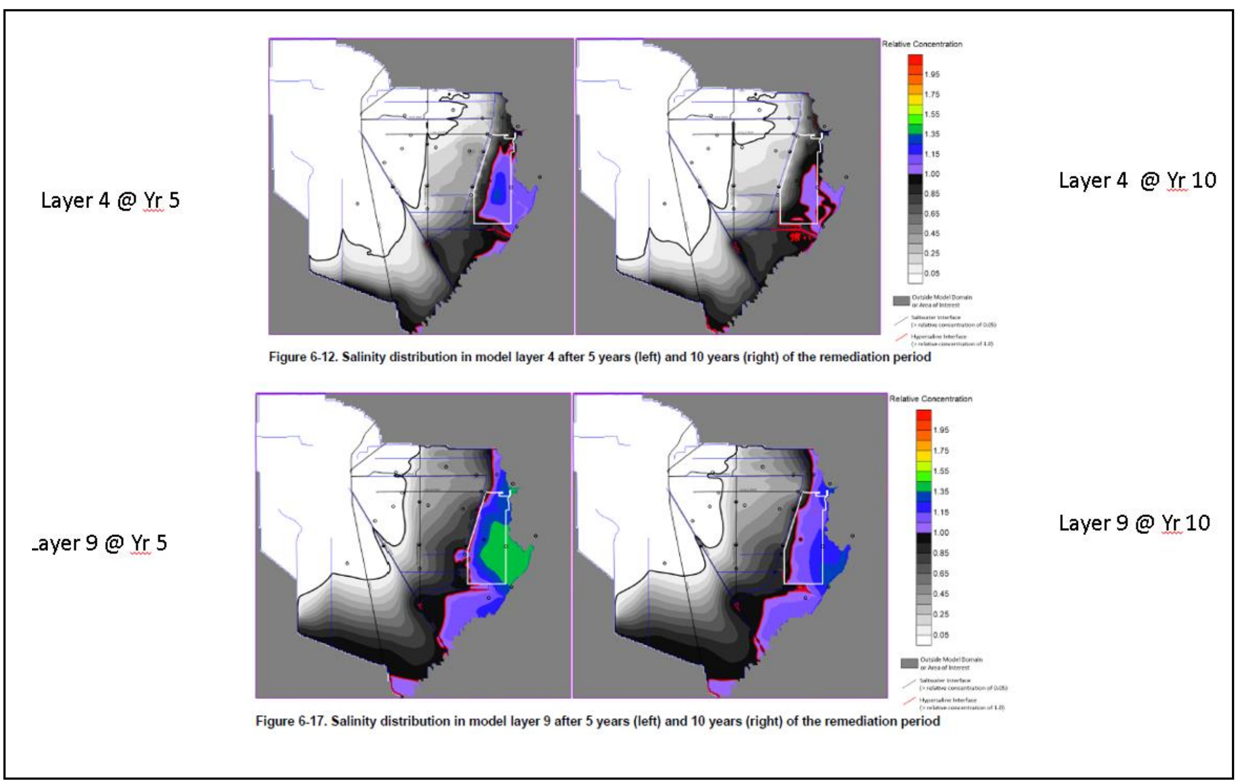

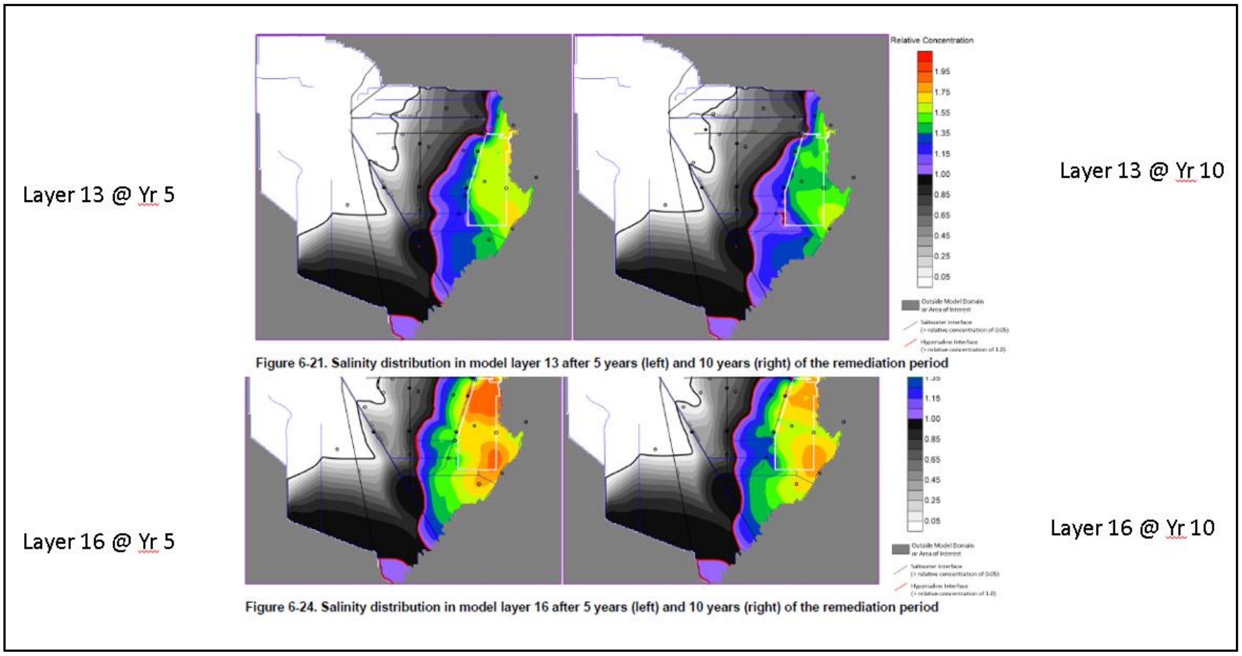

Figure 4-7: Selected layers of Predicted Plume after years 5 (2023) and 10 (2028) of remediation.

Model simulated hypersaline plumes in selected model layers are shown in **Figures 4-6 and 4-7** based on FPL RAASR Yr 4. These results of the modeling simulation clearly indicate that a larger portion of the hypersaline plume will remain west of the FPL's property in the deep Biscayne aquifer by May 2028, the deadline defined in the MDC CA and FDEP CO.

(6) Water Quality Data

A comparison of the plume extents at different time provides an informative means for assessing the progress of the groundwater recovery system. The most reliable data for plume extent delineation would be field-measured water quality data. However, the delineation of a complete hypersaline plume is limited by the availability of direct measurements.

Among the available monitoring wells, TPGW-18 is located at the edge of the hypersaline plume. The water quality change at this location provides direct evidence of the plume retraction. The field-measured chloride concentration values in the middle of 2022 indicate the field-measured chloride concentration is still above 19,000 mg/L as shown in **Table 4-3** below.

Table 4-3: Measured chloride concentration at TPGW-18 (FPL 2022)

DATE	TPGW-18S	TPGW-18M	TPGW-18D
3/1/2018	14200	25200	26400

6/1/2018	12100	24100	24100
9/1/2018	8660	23300	24600
12/1/2018	6510	22700	23500
3/1/2019	7680	24800	25400
6/1/2019	7080	23100	24200
9/1/2019	5620	24000	24500
12/1/2019	6100	23600	23400
3/1/2020	5620	22200	22500
6/1/2020	5620	22500	23200
9/1/2020	4780	24400	23300
12/1/2020	4990	23700	23800
3/1/2021	3360	23200	24100
6/1/2021	3130	20500	21000
9/1/2021	*2810*	*23500*	*23900*
12/1/2021	2610	*22500*	*23200*
3/1/2022	2590	*22200*	*22900*
6/1/2022	2230	*19600*	*22000*

Another key observation is the trend of water quality changes at TPGW-18. **Figure 4-8** shows the change of chloride concentration measured at shallow, middle and deep screens of TPGW-18. The data at the middle and deep screens may suggest a slow decrease of chloride concentration at this monitoring well, but the rate of decrease may raise the concern that the chloride concentration would be lowered to below 19,000 mg/L in five years.

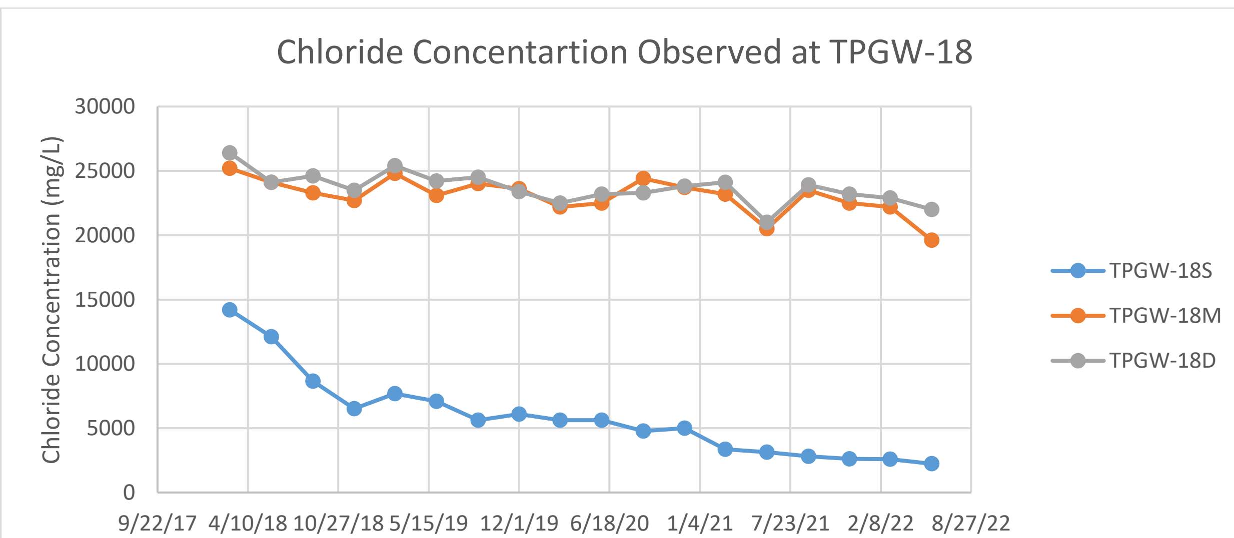

Figure 4-8. Chloride concentration (mg/L) observed at TPGW-18.

Although the success or failure of the RWS cannot be simply judged by the data from one or two monitoring wells, the data from this well, the water quality change TPGW-18 may provide early evidence of the fate of the hypersaline plume due to its unique location.

As discussed in the previous reviews (GTI 2020; 2021; 2022), monitoring well TPGW-18 is located at the edge of the current hypersaline plume so the chloride concentration breakthrough curve at this location may provide us a unique and invaluable opportunity to observe the retraction of the hypersaline plume as a positive indicator of RWS success.

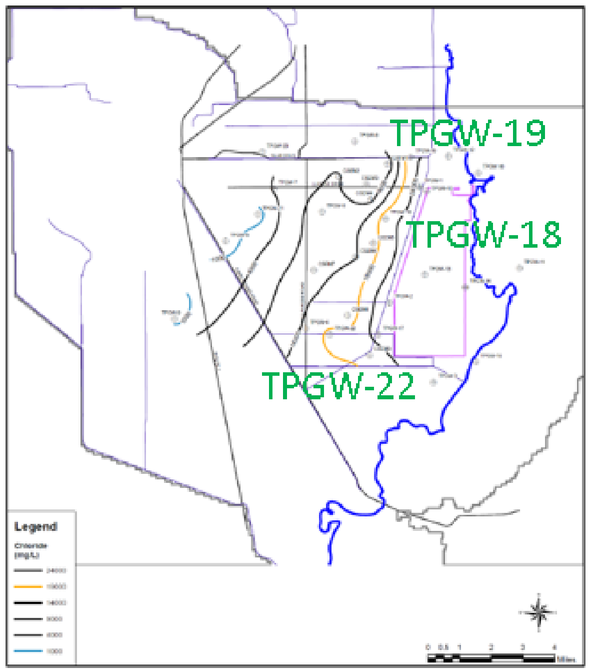

Figure 3.3-3. Groundwater Chloride Contour Map based on 2022 Deep Monitoring Well Data and CSEM Horizon Chloride Values

Deep

Figure 4-9. Groundwater Chloride contours based on 2022 deep monitoring data and CSEM horizon chloride values.

It appears that the 19,000 mg/L chloride concentration contour line bends towards upgradient or west direction at TPGW-18 and TPGW-22 (**Figure 4-9**). The shape of this contour line indicates the groundwater at these two locations are still hypersaline at the deep portion of the aquifer. Because there is no other monitoring well between these two wells, we cannot be sure if the plume has retracted eastward more than these two separate locations. Continuous watch of the breakthrough of chloride concentration at these two locations provide the first-hand evidence whether the remedial goal will be accomplished by o time.

(7) Water Level Contour Maps:

Figure 4-10 shows the water level contour maps for the dry season (April 2022) and the wet season (September 2021) as reported by FPL (2022). FPL mentioned that these two maps were generated manually. The maps indicate the groundwater general flow direction is from west to east towards the Biscayne Bay. However, it is not clear why the contours bend in the dry season under the CCS area where dense connected canals are present. In addition, it is not clear if the water levels are vertically uniform.

The maps also indicate that there is gradient-flat area north of TPGW-18 and west of TPGW-1. If the water levels shown in these maps are similar vertically, could the flat groundwater flow gradient northwest of TPGW-18 explain why the plume eastward movement is relatively slow in the deep portion of the aquifer?

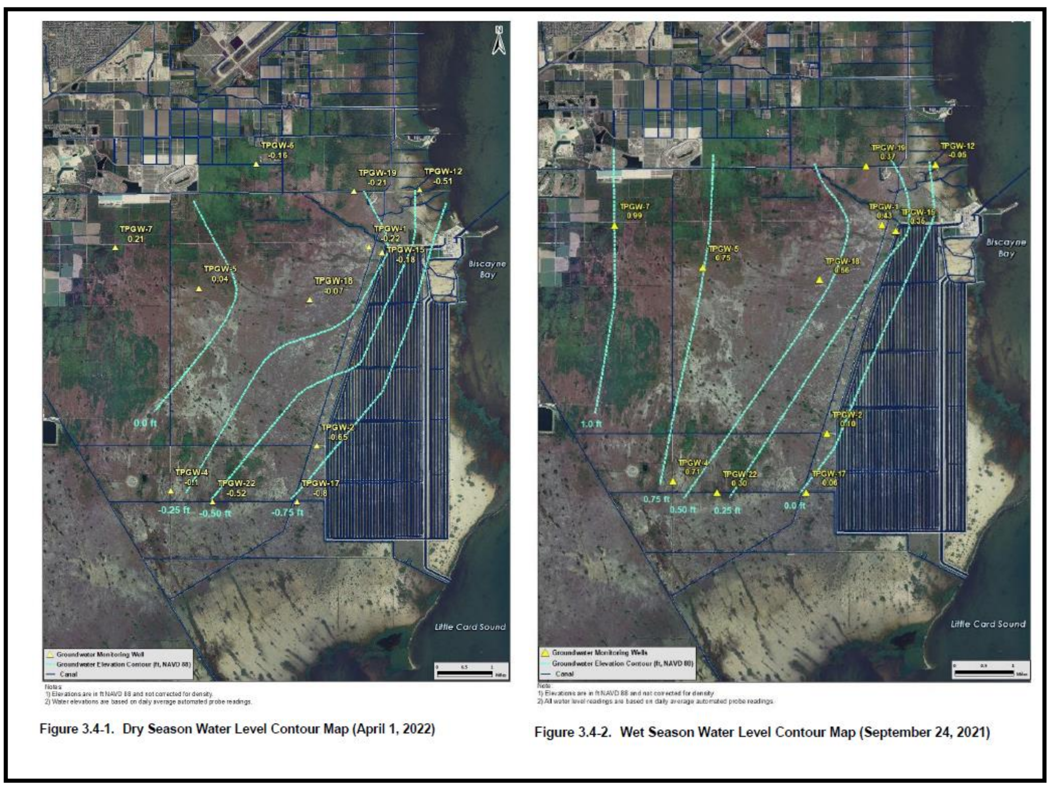

Figure 4-10. Water level contour maps for the dry season (April 2022) and the wet season (September 2021) (FPL 2022).

(8) Relatively Large Errors in Relative Salinity Match

Figure 4-11 shows simulated and observed relative salinity at selected TPGW wells after model calibration. Significant differences can be observed at a few monitoring screens, so further model calibration with a focus on solute transport is necessary to improve the model calibration. Since the salt distribution in the aquifer is also affected by the groundwater heads, further head calibration should also be considered.

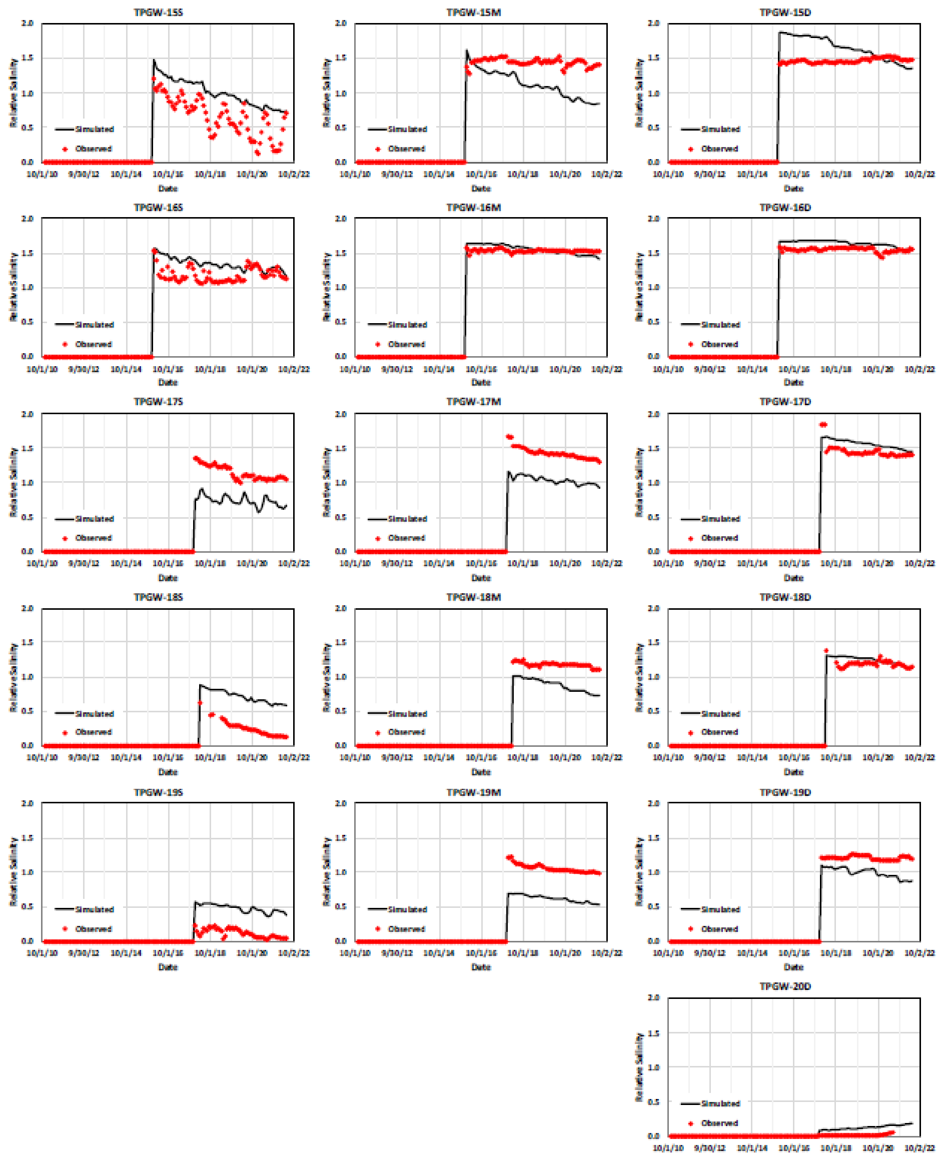

Figure 4-11 Selected simulated and observed relative salinity at selected wells within the model domain for the monthly transient model (FPL 2022: Appen. I: Figure 5-10).

(9) Salt Extraction Rates

The salt extraction rate is a direct indicator of the efficiency of the RWS. So far, the RWS is working well. After 4 years, 9.24 billion lbs. of salt have been removed from the aquifer (FPL 2022). The westward movement of the hypersaline plume has been halted and the plume is either being retracted eastward in the shallow and middle portions of the aquifer or held in the deep portion of the aquifer.

Figure 4-12 shows the monthly salt extraction rate from 2018 to 2022. As shown in the figure, the monthly salt extraction rate has been relatively statable over the last four years at about 140 million ponds. As the remediation continues, a decline of the monthly salt extraction rate is expected when the shallow and middle of the aquifer become less salty, as shown in **Figure 4-13**. It is not clear at this point why the salt extraction rate was relative stable yet the salinity in the shallow and middle portions of the aquifer declined over time. One possible explanation is that the RWS mainly extracts salt from the deeper portion where the hypersaline conditions remain. This would be the ideal situation when the RWS are removing the hypersaline plume west of the CCS.

Another possibility is that the RWS wells are getting their water from the CCS area where water is hypersaline. Under this condition, the remediation efficiency is not optimized since part of RWS capacity is used to withdraw the water from the CCS.

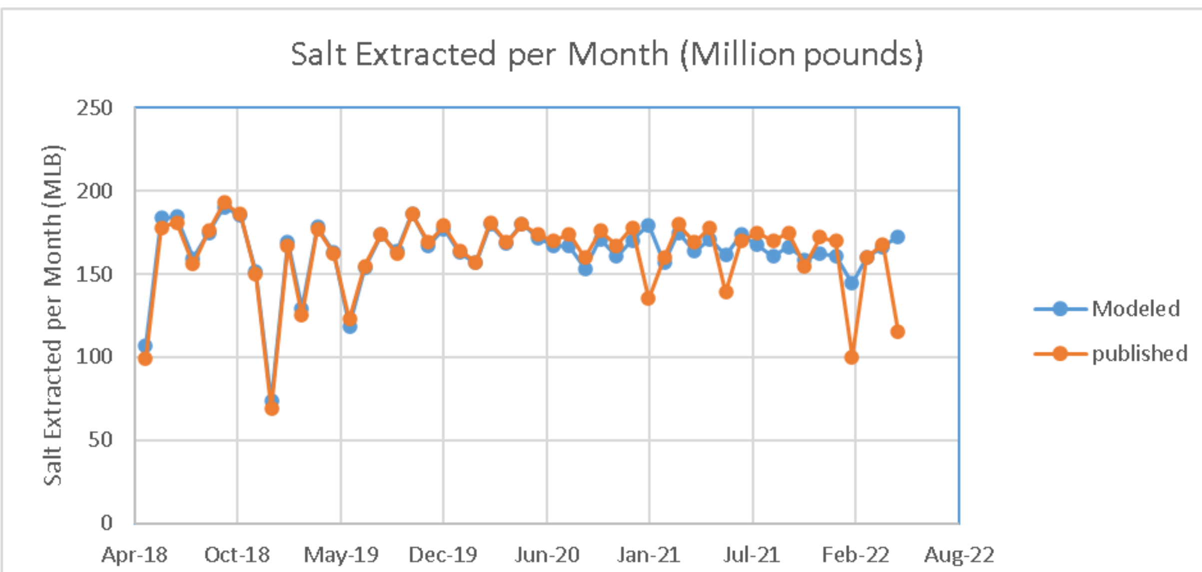

Figure 4-12. Monthly salt extraction (mlb) of the RWS system.

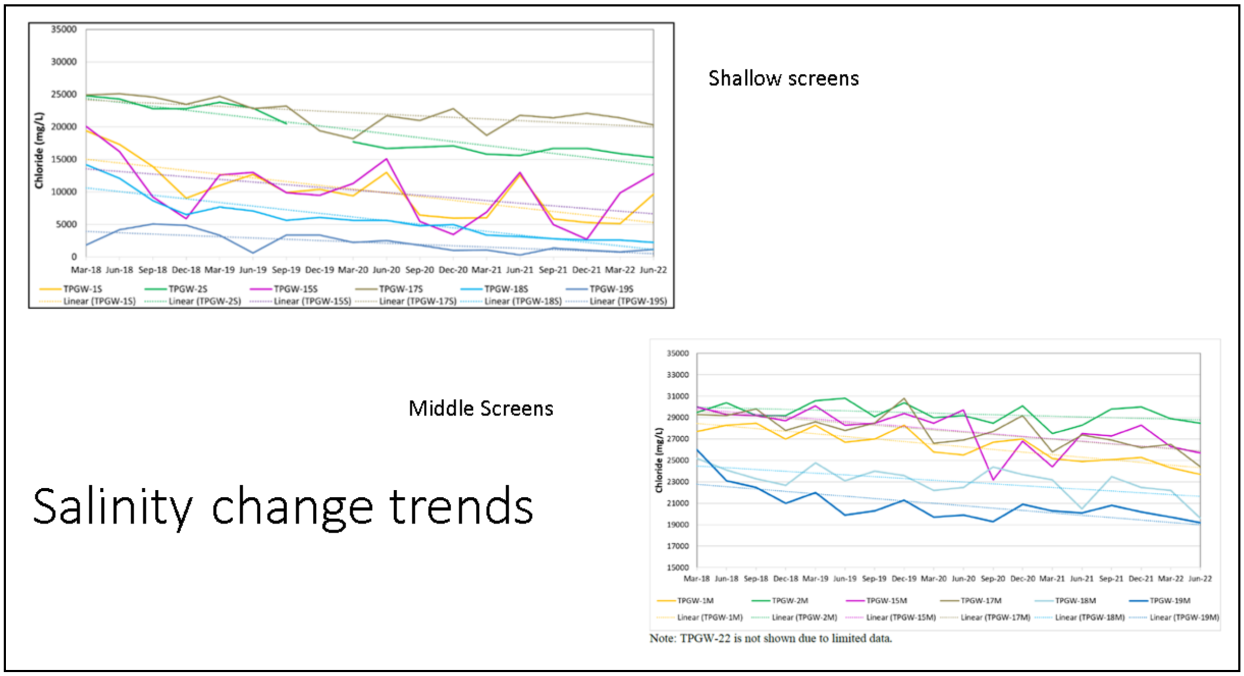

Figure 4-13. Trends of chloride concentration at selected TPGW monitoring wells.

Figure 4-14 shows the model-predicted salinity change in next 6 years (from 2022 to 2028) for each of the RWS well (FPL 2022). The salt extraction rate at RWS-1 seems to be relatively low but statable. The salt extraction rates of other RWS wells appear to be in a slow but steady decline trend.

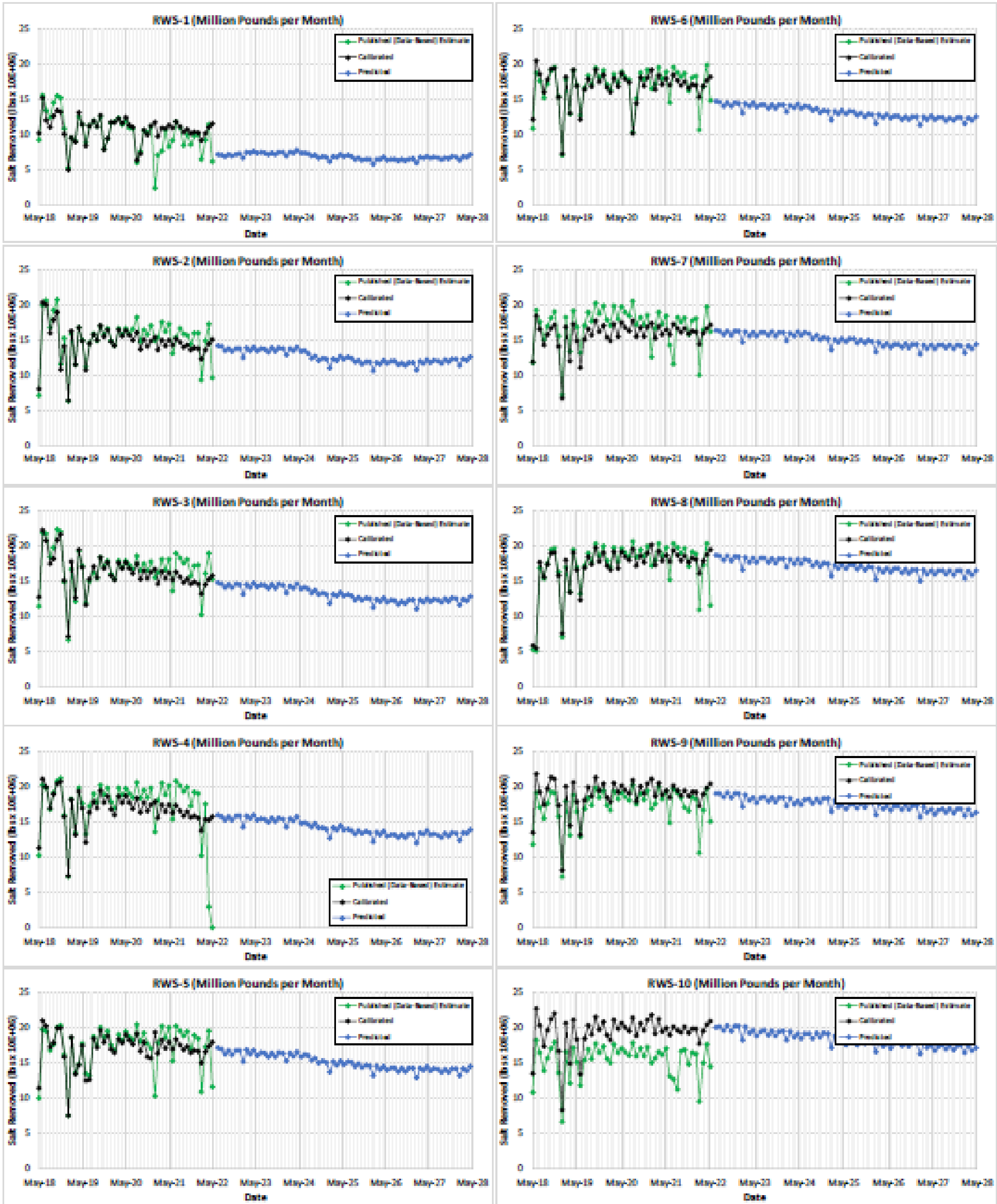

Figure 6-6. Predicted mass extracted by well for 10-year remediation period

Figure 4-14. Predicted mass extracted by RWS wells for 10-year remediation period (FPL 2022).

Model-predicted total monthly salt extraction rates of the RWS wells from 2022 to 2028 are shown in **Figure 4-15**. It appears that monthly total salt extraction rate dops relatively fast from 150 million pounds to 140 million pounds from 2024 to 2026 then the rate change becomes relatively small.

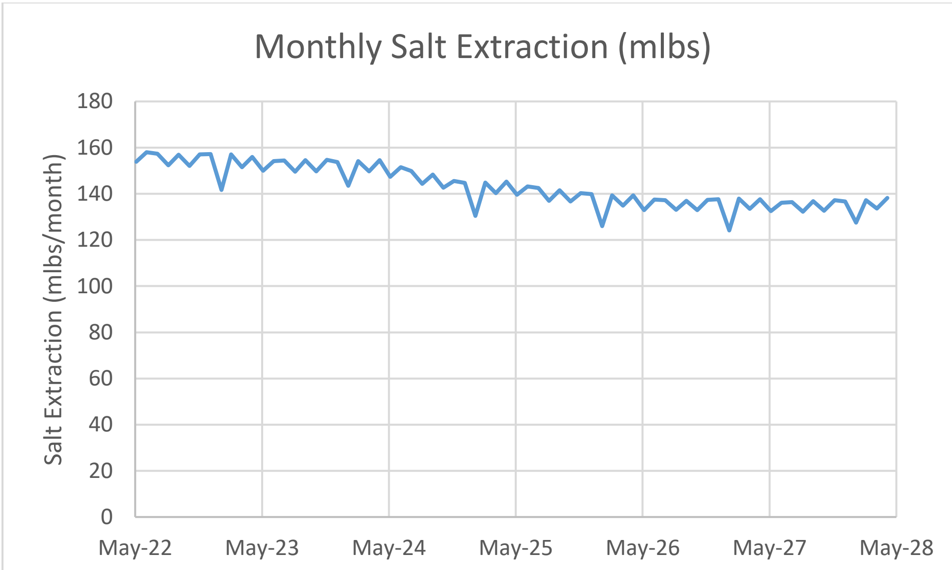

Figure 4-15. Model-predicted monthly salt extraction rates from 2022 to 2028.

It is interesting to check modeled relative salinity of extracted water. The average salinity of pumped water can be estimated by the monthly total salt extracted and pumping rate for the same time period with proper unit conversions. The estimated salinity of pumped water from 2022 to 2028 is shown in Figure **4-16**.

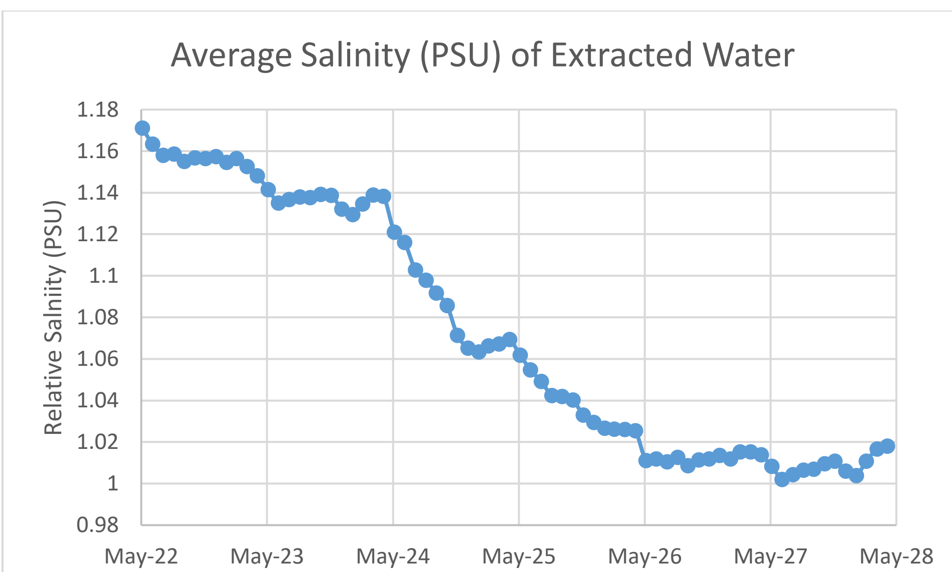

Figure 4-16. Average relative salinity of extracted water by the RWS wells.

Based on Figure 4-16, the average salinity of pumped water is expected to drop more quickly between 2024 and 2026. This would be a good sign indicating the possible retraction of the hypersaline plume. However, another possibility is that the decrease of the salinity is only a local phenomenon, if the RWS wells obtain a significant portion of pumped water from shallow layers. Therefore, identification of the sources of water feeding the RWS wells may help us understand the fate of the hypersaline plume and efficiency of the current remediation system. Thus, it is our recommendation to perform some backward particle tracking analysis for the extraction wells.

Figure 4-16 shows that at the end of the 10-year RWS operation, relative the salinity of pumped water is still above 1.0, as an indicator of existence of hypersaline water outside of the FPL property.

(10) Gaps in Capture Zones

It appears that there are gaps (circled areas in **Figure 4-17**) in capture zones between RWS-7 and its neighboring RWS wells (RWS-6 and RWS-8). These gaps in capture zones were concerning (GTI 2021). FPL investigated these gaps and indicated that "particles in this area are either stagnant, appear to oscillate in direction with no clear destination, or traverse along circuitous pathways that require travel times of greater than 10 years to reach their final RWS well destination." FPL suggested that "The gaps between capture zones in lower layers are not indicative of lost particles or loss of containment. Rather, groundwater in between some RWS wells follow circuitous, seasonally dependent flow paths that neither terminate at an RWS well (e.g., many particles end up in the CCS) nor contribute to the western migration of the hypersaline interface." (FPL 2022 p.6-2).

The capture zones of these RWS wells remain the focus of this study since these wells are a key component of the remedial system. A common method of capturing zone delineation is to perform backward particle tracking analysis. Backward particle tracking from the screens of these wells may be helpful in identifying the source of the water and contribution of the water from different portions of the aquifer to the RWS wells. This exercise may be also helpful to verify the conceptual model and explain why the hypersaline plume in the deep aquifer is slow to move.

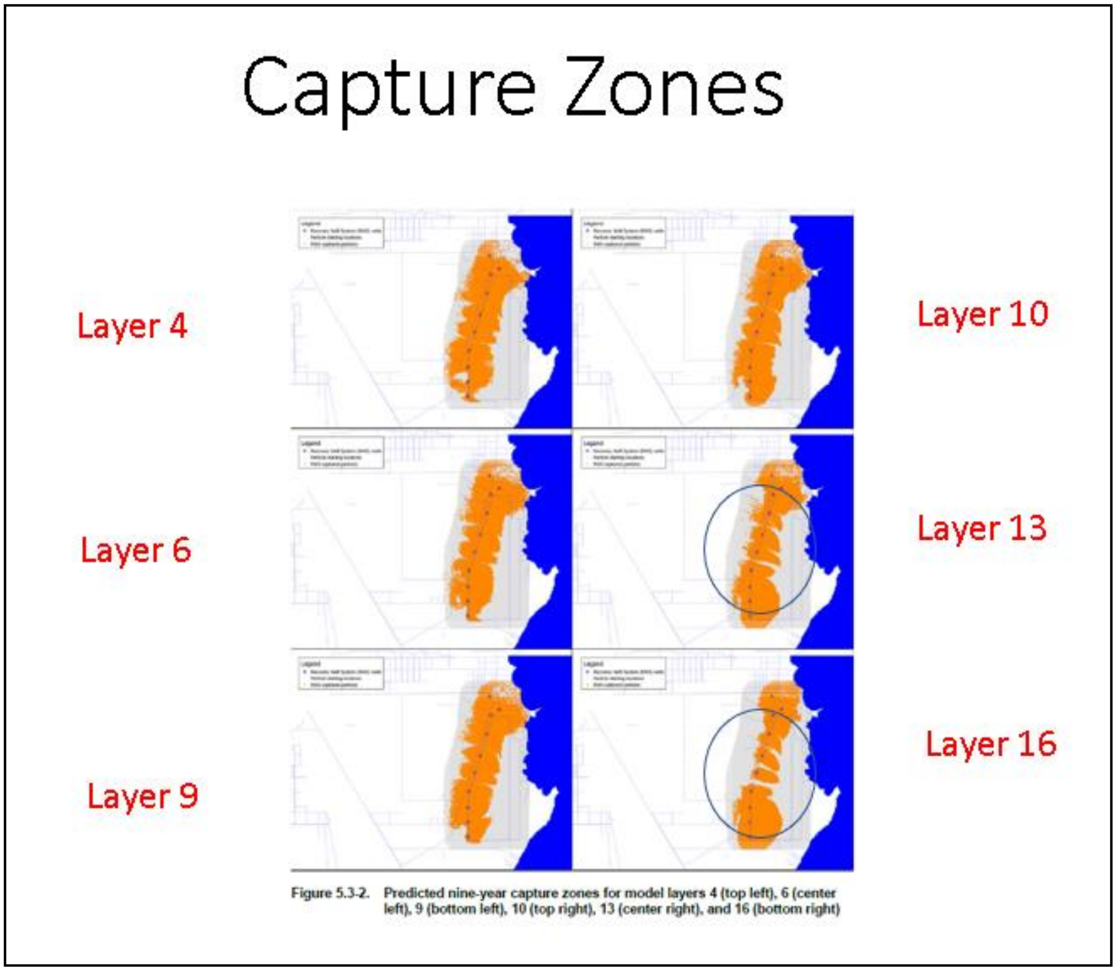

Figure 4-17: Predicted capture zones of the RWS wells at selected model layers.

(11) Assessment of Remediation Goals of The MDC CA

The main objective of the RWS is to retract the hypersaline plume in the Biscayne aquifer to the FPL property (east of 1-31E) by May 2028. Due the model's inability to predicting the plume movement, it remains difficult to provide a confident assessment of whether the existing remediation system will retract the hypersaline plume to the FPL's property on time. Based on the modeling results and groundwater monitoring data, it seems this objective will likely be met in the shallow and middle zones of the aquifer but not certain for the deep Biscayne aquifer. Both the modeling and groundwater monitoring data indicate that the RWS is less efficient for the deep aquifer.

(12) Alternative Remediation Methods

Additionally, to predict plume movement, scenario evaluation is another major model application commonly used. Scenario evaluation and comparison allow selection of the best scenario among different options. Once a model is developed, even if it may not perfectly be calibrated, it will be a quick exercise to test and compare different options under similar conditions.

Different additional remediation scenarios, focusing on retracting the plume in the deep aquifer, may be considered and assessed in the model. Only less than five years are left to retract the plume completely to FPL's property to comply with MDC CA, and it might be the time to consider how to enhance the existing RWS. Since it takes time to assess, select, permit, and build an alternative or additional remediation measures, it may be better to consider additional remediation measures now.

Evaluation of alternative scenarios also provides an opportunity to test, verify, and improve the conceptual model for this model.

5. Findings, Conclusions and Recommendations

5.1 Findings and Conclusions

(1) The current RWS is making progress as indicated by CSEM survey data and groundwater monitoring data. About 9.24 billion pounds of salt has been removed from the aquifer since the beginning of the RWS operation and approximately 2.37 billion pounds of salt was removed in this report time period. The progress is more pronounced for the shallow and middle portions of the aquifer. The CSEM survey data from 2018 to 2022 indicated that the expansion of the hypersaline plume has been halted or reversed in the shallow portion of the aquifer. Water quality data from groundwater monitoring wells, also showed the decline of chloride concentration at many monitoring well sites.

(2) One of the major changes of FPL SEAWAT model version 7 from previous versions is the increase of vertical resolution by splitting the deeper model layers. The current model has 17 layers, increased from 11 layers in previous models. The deep high flow zone in the previous models is split to the upper portion and the lower portion of the deep high flow zone. The increase of model layers helps more accurately locate the screens of monitoring wells and extraction wells. However, the increase of the model layers does not appear to change the overall picture of the model simulations. The most prominent difference appears to be at TPGW-1 in model layer 13 (Layer 10 in previous models), where simulated plume extent is much closer to the L-31E canal based on the current version of SEAWAT model.

(3) Based on the provided calibration statistical summary for this version of the SEAWAT model, the model has been reasonably well-calibrated to the calibration targets. The model was developed with good modeling practices. The model has gone through a number of steps of calibration against the data from many years. Automatic calibration tool (PEST) was implemented to facilitate the model calibration. The calibration targets include water levels, salt concentration, CSEM survey data, historical saltwater intrusion freshwater/saltwater interface, and monthly salt extraction rates. The model- predicted water levels, monthly salt extraction rates, and salinity in most of monitoring wells as well as selected CSEM survey data were in close agreement with the observed data. The solute transport calibration has room for improvement in future model calibration. The model-predicted salinity values at some of the monitoring wells are not in close agreement with field measurements.

(4) Further model calibration with focus on the historical salinity match is necessary. The match between modeled and observed data at a number of monitoring wells is not satisfactory and needs to be improved. Modeled and CSEM-based plume extents in deep aquifer are not in close agreement for May 2018, which presented an initial mass concentration distribution. The results from the sensitivity analysis indicate that externally generated initial mass conditions may not work well with

prediction model, so a set of simulated initial conditions (heads, mass and temperature) may be necessary for prediction model improvement.

(5) The current version of SEAWAT model did not match the plume extents in the deep layers, representing the deep portion of the Biscayne aquifer. Comparison of modeled plume extent after model calibration and the CSEM-based plume extents in deep model layers indicate that the model is not able to match the field conditions for May 2022, which represent the initial condition for the prediction model.

(6) The model's inability for prediction of future change of the hypersaline plume remains as the major concern. The model did not match the plume in deep layers as of the end of May 2022 and the current model prediction indicates the hypersaline plume in the deep portion of the aquifer would not be retracted to the FPL's property by May 2028.

(7) The modeling results from the sensitivity simulation indicate that the hypersaline plume unintuitively expands westward in model layer 16, which is contrary to the conceptual model, and it is not supported by the CSEM survey data. On the other hand, this sensitivity simulation provides useful information that may allow us to identify some problems in the current conceptual model. The results of the sensitivity analysis may suggest that externally generated initial mass concentration may not hydrodynamically balanced with the model. Therefore, efforts to match the salinity distributions prior to the operation of the RWS (April 2018) may be critical to improve the model's ability for prediction. If the model cannot match the salinity distribution in April 2018, it will be very difficult to be used to predict the fate of the hypersaline plume with reasonable confidence.

(8) TPGW-18 is located at the edge of the hypersaline plume so the change of salinity at this location is a valuable indicator of the effectiveness of the RWS. So far, the water quality data from this well has not shown a convincing trend in the middle and deep sections. The chloride concentration contour maps, based on measured chloride concentrations have indicated the plume retraction is slightly behind at TPGW-18 and TPGW-22 in deep aquifer. The changes of salinity in the vicinity of TPGW-18 and TPGW-22 need to be closely watched. Although data from these two points may not be representative of the entire progress of remediation, they do provide critical data to provide us with the first hand of break-through curves showing the retraction of the plume in the deep aquifer.

(9) FPL has performed a sensitivity analysis to investigate the hydrological impact of L-31E Canal to the RWS system by modeling the canal as a drain rather a river feature. The results indicate the plume retraction are not significantly different for the shallow and middle portions of the aquifer. The results of this sensitivity analysis suggests that remedial efficiency of the RWS wells may be sensitive to the availability of water from the shallow layers above. The impact to the hypersaline plume is weaker at deeper depth such as model layer 16.

(10) The salt extraction rate is a direct indicator of the efficiency of the RWS. The modeled monthly salt extraction rates have been in close agreement of published data from 2018 to 2022. The simulated monthly salt extraction rate has been relatively statable over the last four years at about 140 million pounds per month. As the remediation continues, a decline of the monthly salt extraction rate is expected when the shallow and middle of the aquifer become less salty. It is not clear at this point why the salt extraction rate was relative stable yet the salinity in the shallow and middle portions of the aquifer declined over time. One possible explanation is that the RWS mainly extracts salt from the deeper portion where the hypersaline conditions remain. This would be the ideal situation when the RWS are removing the hypersaline plume west of the CCS but not from the CCS area. Identification of the sources of water feeding the RWS wells may help us understand the fate of the hypersaline plume and efficiency of the current remediation system. Thus, it is our recommendation to perform some backward particle tracking analysis for the extraction wells.

(11) It appears that there are gaps in capture zones between RWS-7 and its neighboring RWS wells (RWS-6 and RWS-8). The capture zones of these RWS wells remain the focus of this study since these wells are a key component of the remedial system. Backward particle tracking from the screens of these wells may be helpful in identifying the source of the water and contribution of the water from different portions of the aquifer to the RWS wells. This exercise may be also helpful to verify the conceptual model and explain why the hypersaline plume in the deep aquifer is slow to move.

5.3 Suggestions/Recommendations

(1) Further model calibration is recommended with focus on the salt transport. Although the calibration statistics of the current model calibration has showed the model generally matched the water level and salinity at calibration targets, additional calibration with focus on salt transport is recommended. Match of modeled and observed chloride concentration at some TPGW wells need to be improved, especially for the screens at deep aquifer.

(2) There is an urgent need to solve the model calibration problem associated with the model's inability to match the past and current locations of the plume extents. If the model cannot match the existing conditions, any predictions should be interpreted with caution. Development of a set of hydraulically balanced initial conditions (head, mass concentration and temperature) may be a key task for improvement of model predictions. The modeling results from the sensitivity may suggest that an externally generated initial mass concentrations may not work properly with the model.

(3) Backward particle tracking analysis from the RWS wells is recommended, combined with mass balance evaluation, for identification of the sources of water feeding the RWS wells.

(4) Additional sensitivity analyses are suggested for better for better understanding of the hydrogeological dynamics of the system and fate of the hypersaline plume. Additional sensitivity analyses include test of regional gradients, vertical hydraulic connections between the middle and lower high flow zones, effective porosity, etc.

(5) Different additional remediation scenarios, focusing on retracting the plume in the deep aquifer, may be considered and assessed using the model. Only less than five years are left to retract the plume completely to FPL's property to comply with MDC CA, and it might be the time to consider how to enhance the existing RWS so the remediation goals can be met by May 2028. Since it takes time to assess, select, permit, and build an alternative or additional remediation measures, it may be better to consider other options to enhance the remediation. Evaluation of alternative scenarios also provides an opportunity to test, verify, and improve the conceptual model for this model.

6. References

Chin, D., 2016. The cooling-canal system at the FPL Turkey Point power station: https://www.miamidade.gov/environment/library/reports/cooling-canal-system-at-the-fpl-turkey-point-power-station.pdf.

Florida Power &Light (FPL), 2019. FPL Turkey Point Remedial Action Annual Status Report (RAASR) Year 1, November 15, 2019.

Florida Power &Light (FPL) 2020a. Florida Power & Light Company Turkey Point Clean Energy Center Power Plant Site Certification No. PA 03-45 Petition for Modification F Supplemental Salinity Management Plan, response to FDEP RAI, October 9, 2020.

Florida Power &Light (FPL) 2020b. Turkey Point Clean Remedial Action Annual Status Report (RAASR) Year 2 and The variable Density Groundwater Flow and Solute Transport Model (v5), November 13, 2020.

Florida Power &Light (FPL) 2021. Turkey Point Clean Remedial Action Annual Status Report (RAASR Year 3) and The Variable Density Groundwater Flow and Solute Transport Model (version 6), November 15, 2021.

Florida Power &Light (FPL) 2022. Turkey Point Clean Remedial Action Annual Status Report (RAASR Year 4) and The Variable Density Groundwater Flow and Solute Transport Model (version 7), November 15, 2022.

Groundwater Tek Inc. (GTI): 2020. Review of FPL's Groundwater Flow and Salt Transport Models and Assessment of the First Year Operation of the RWS, *prepared for* Division of Environment and Resources Management Miami-Dade County, Fl., Naples, Florida; July 2020.

Groundwater Tek Inc. (GTI): 2021. Review of FPL's RAASR Year 2 and The Variable Density Groundwater Flow and Salt Transport Models (v5), *prepared for* Division of Environment and Resources Management Miami-Dade County, Fl., Naples, Florida; July 2021.

Groundwater Tek Inc. (GTI): 2022. Review of FPL's RAASR Year 3 and The Variable Density Groundwater Flow and Salt Transport Models (v6), *prepared for* Division of Environment and Resources Management Miami-Dade County, Fl., Naples, Florida; Feb. 2022.

Guo, W. and C. D. Langevin, 2002. User's guide to SEAWAT, A Computer Program for Simulation of Three-dimensional Variable Density Groundwater Flow, Techniques of Water-Resources Investigations of the U.S. Geological Survey, Book 6, Chapter 7.

Langevin, C.D., Thore, D.T., Dausman A.M., Sukop, M.C., and Guo, W., 2008. SEAWAT Version 4: A Computer Program for Simulation of Multi-Species Solute and Heat Transport: USGS Techniques and Methods Book 6, Chapter A22, 39 p.

Miami-Dade County (MDC) Department of Regulatory and Economic Resources (RER), Division of Environmental Resources Management (DERM). 2015. Consent Agreement between Miami-Dade County and Florida Power & Light Company. October 7, 2015.

South Florida Water Management District, 2013. Letter from Terrie Bates, Director, Water Resource Division, to Barbara Linkiewicz, FPL & NextEra Energy Resources, Juno Beach, Florida, regarding Units 3 and 4 Post-Uprate Monitoring (reduction of groundwater/surface water monitoring). June 3, 2013.